ACT-24
CERN-TH-5853/90
CTP-TAMU-96/90

ASTROPHYSICAL CONSTRAINTS ON MASSIVE UNSTABLE NEUTRAL RELIC PARTICLES

John Ellis
Theoretical Physics Division - CERN
1211 - Geneva 23, Switzerland

G.B. Gelmini
Department of Physics, University of California
Los Angeles, CA 90024-1547, U.S.A.

Jorge L. Lopez [1] and D.V. Nanopoulos [2]
Center for Theoretical Physics, Department of Physics
Texas A & M University
College Station, TX 77843-4242, U.S.A.
and
Astroparticle Physics Group
Houston Advanced Research Center (HARC)
The Woodlands, TX 77381, U.S.A.

Subir Sarkar
Department of Theoretical Physics
University of Oxford
Oxford OX1 3NP, England

Abstract

There has recently been renewed interest in massive neutral dark matter particle candidates with masses greater than $\sim$ 1 TeV which may be unstable. We reevaluate the constraints on such particles from the possible effects of their decays on the spectrum of the microwave background radiation and the primordially synthesised abundances of the light elements, from observations of the diffuse gamma-ray background radiation, and from searches for muons and neutrinos in nucleon decay and cosmic ray detectors. We find that such unstable neutral relics may well have the cosmological critical density if their lifetime exceeds $\sim 10^{16}$ yr. We illustrate our arguments by applying them to technicolour baryons and to 'cryptons' in superstring-inspired models.

ACT-24
CERN-TH-5853/90
CTP-TAMU-96/90
December 1990

---

1) Supported by an ICSC-World Laboratory Scholarship.
2) Supported in part by DOE Grant DE-FG05-91-ER-40633.

1 Introduction

Astrophysicists assure us that most of the matter in the Universe — at least $\approx 90\%$, and possibly even $\approx 99\%$ — does not shine [1]. This suggests *a priori* that the relic particles which constitute the dark matter are electromagnetically neutral. Another indication that such particles are unlikely to have electromagnetic or strong interactions comes from the failure of terrestrial searches for anomalously heavy isotopes of various elements, with masses up to ~ 10 TeV [2]. Dark matter particles with strong or electromagnetic interactions would presumably have bound with ordinary nuclei now present on Earth and should therefore have shown up in these searches at a level far above the experimental sensitivities. We infer that dark matter particles are either neutral and/or very heavy [3].

There has recently been a resurgence of interest in charged massive dark matter particles, and various constraints on this possibility have been identified [4]. The most severe of these is that apparently imposed by the continued existence of neutron stars, which indicates that such particles do not congregate inside them sufficiently to form black holes which would swallow up their hosts [5]. Although it may be possible to evade this constraint, a more likely constituent of the dark matter appears to be a neutral particle. There are many such candidate particles with masses $\sim 10 - 100$ GeV, such as massive neutrinos or the lightest supersymmetric particle [3]. However these are increasingly constrained by measurements of the Z^0 decay width at *LEP*, and in some cases excluded altogether [6]. For this reason, and also for those described earlier, it is now pertinent to consider yet more massive neutral particles as possible constituents of the dark matter.

Indeed, at least two such candidate particles have recently attracted theoretical interest on their own merits, *viz.* the lightest technicolour baryon [7], which is expected to have a mass of $\mathcal{O}$(TeV), and the lightest 'crypton', or bound state in the hidden sector of a superstring-derived model [8], which could have a mass of $\mathcal{O}(10^{10})$ GeV.[1] Both of these candidates are expected to be unstable, although very likely with a lifetime exceeding the age of the Universe. Now therefore is an opportune moment to reconsider the astrophysical and cosmological constraints on such massive *unstable* neutral relic particles.

For short lifetimes, we consider the bounds from the possible alteration of light element abundances, both through the direct effect of the decaying particles on primordial nucleosynthesis and, more importantly, through the effects of the decay products on the synthesised elements. We also discuss the bounds from the possible distortion of the spectrum of the cosmic microwave background radiation by particle decays occuring before the recombination era. For longer lifetimes, the decay products contribute to the diffuse background radiations and are constrained by observations of the isotropic gamma-ray background as well as limits on high energy muons and neutrinos in nucleon decay detectors and cosmic ray air shower arrays. Finally, we discuss the constraints thus imposed on particle physics models.

[1] It has been argued that no stable relic particle may have a mass in excess of ~ 340 TeV [9]. However this bound does not apply to cryptons since there is likely to be significant generation of entropy *after* their self-annihilations go out of thermal equilibrium [8].

2 Bounds from Primordial Nucleosynthesis

The canonical model of Big Bang nucleosynthesis [10] assumes that the Universe was 'radiation-dominated' by relativistic particles (photons, 3 massless ν types and, for $T \gtrsim m_e$, e^+e^- pairs) during the epoch of primordial nucleosynthesis ($t_{ns} \approx 10^2$ sec) and predicts yields of the light elements D, ^3He, ^4He and ^7Li which agree with their observationally inferred primordial values [11,12], for a relatively narrow range of the nucleon-to-photon ratio, $\eta \equiv n_N/n_\gamma \sim 10^{-10} - 10^{-9}$. The presence during nucleosynthesis of an additional massive *non-relativistic* particle would increase the energy density, hence the rate of expansion, and lead to a change (generally an increase) in the synthesised abundances. (This effect is different from that due to the addition of a new *relativistic* particle since the particle energy density is now $\propto T^3$ rather than $\propto T^4$.) Additionally, if the particle decays during or after this epoch into photons or charged particles, the nucleon-to-photon ratio decreases [2]. This can be used to constrain the decaying particle abundance in the following manner.

The observationally-inferred upper limit [3] on the mass fraction of primordial helium, $Y_p(^4He) < 0.25$, imposes an *upper* bound on $\eta_{ns} \equiv \frac{n_N}{n_\gamma}|_{t_{ns}}$, the nucleon-to-photon ratio during the nucleosynthesis epoch, while observations of luminous matter in the Universe [4] set a *lower* bound on the same ratio today, $\eta_0 \equiv \frac{n_N}{n_\gamma}|_{t_0}$. Hence one can require the particle decays not to have decreased η by more than a factor η_{ns}/η_0, having calculated the elemental yields (and η_{ns}) taking into account the increased expansion rate due to the presence of the decaying particle.

If we assume that all the unstable x particles decay simultaneously when the age of the Universe t equals the particle lifetime τ_x and dump a fraction f_γ of their energy density ρ_x into photons, then the resultant change in η is [16]

$$\frac{\eta_{before}}{\eta_{after}} = \left(\frac{f_\gamma g_* T_m}{2T_d}\right)^{\frac{3}{4}} \leq \frac{\eta_{ns}}{\eta_0} \qquad \text{for} \qquad T_m \gg T_d\,, \tag{1}$$

where T_d is the blackbody photon temperature T at decay ($t = \tau_x$) obtained from the time-temperature relationship

$$t = -\int \left[\frac{3M_P^2}{8\pi(\rho_x + \rho_{rel})}\right]^{\frac{1}{2}} \frac{dT}{T} = \left(\frac{5}{g_*\pi^3}\right)^{\frac{1}{2}} \frac{M_P}{T_m^2}\left[\left(\frac{T_m}{T} - 2\right)\left(\frac{T_m}{T} + 1\right)^{\frac{1}{2}} + 2\right]. \tag{2}$$

[2] This requires thermalisation of the released energy which is very efficient for decay lifetimes $\lesssim 10^5$ sec. For longer lifetimes thermalisation is incomplete, but this allows even stronger constraints to be derived from the relic photon spectrum (see §3).

[3] This is obtained from the recently quoted value [12] $Y_p(^4He) = 0.235 \pm 0.004$ (statistical), to which we have added an estimated [13] systematic error of ± 0.01.

[4] The luminous regions of spiral and elliptical galaxies have mass-to-light ratios in the range $\sim (8 - 20)\ h\ [M/L]_\odot$ [14], whereas critical density would correspond to a ratio $(M/L)_c \simeq 1500^{+700}_{-400}\ h\ [M/L]_\odot$ [15]. Thus a lower limit to the fraction of the critical density in nucleons is $\Omega_N \gtrsim 0.01$, which implies $\eta_0 \simeq 2.81 \times 10^{-8}\Omega_N h^2 (T_0/2.7^0\mathrm{K})^{-3} \gtrsim 6 \times 10^{-11}$, for a present Hubble parameter h ($\equiv H_0/100$ Km sec^{-1} Mpc^{-1}) > 0.5 and a present blackbody photon temperature $T_0 < 2.8^0$K.

Here, T_m is the temperature at which the massive particle begins to 'matter-dominate' the Universe, given by the condition $\rho_x(T_m) = \rho_{rel}(T_m)$, *i.e.*

$$m_x n_x(T_m) = \frac{\pi^2 g_*}{30} T_m^4 , \tag{3}$$

where g_* is the number of relativistic degrees of freedom (= 10.75 for $m_\mu \gtrsim T \gtrsim m_e$, and $\simeq 3.36$ for $T \lesssim m_e$).

From eq. (2) we obtain $\tau_x \propto T_m^{-\frac{1}{2}} T_d^{-\frac{3}{2}}$ for $T_m \gg T_d$ (*i.e.* if the x particles decay well after the Universe has become dominated by their energy density). In this approximation, the constraint on the decay lifetime is [16]

$$\tau_x \lesssim 0.8 \text{ sec } f_\gamma^{-\frac{3}{2}} \left(\frac{T_m}{\text{MeV}}\right)^{-2} \left(\frac{\eta_{ns}}{\eta_0}\right), \tag{4}$$

taking $g_* = 3.36$, *i.e* assuming $T_d \ll m_e$.

As mentioned above, the upper bound on η_{ns} corresponding to the observational requirement $Y_p(^4He) < 0.25$ depends on the extent to which the expansion rate during nucleosynthesis is influenced by the massive particle. Kolb & Scherrer [17] have numerically computed the effect on the elemental yields when a non-relativistic neutrino with a specified energy density is present. Their results indicate that $\eta_{ns} \propto T_m^{-\frac{1}{2}}$ for $T_m \gtrsim 10^{-2}$ MeV and $\eta_{ns} \sim$ constant for $T_m \lesssim 10^{-2}$ MeV. Using the actual values of η_{ns} obtained by these authors, Ellis, Nanopoulos & Sarkar [18] obtained the following restrictions on the energy density of the decaying particle as a function of its lifetime:

$$\left(\frac{m_x}{\text{GeV}}\right)\left(\frac{n_x}{n_\gamma}\right) \lesssim 3.3 \times 10^{-3} \left(\frac{\tau_x}{\text{sec}}\right)^{-\frac{1}{3}} f_\gamma^{-\frac{1}{2}} \left(\frac{\eta_0}{6 \times 10^{-11}}\right)^{-\frac{1}{2}}$$
$$\text{for } t_{ns} \lesssim \tau_x \lesssim 3.8 \times 10^5 f^{-\frac{1}{2}} \text{ sec},$$
$$\lesssim 2.8 \times 10^{-2} \left(\frac{\tau_x}{\text{sec}}\right)^{-\frac{1}{2}} f_\gamma^{-\frac{3}{4}} \left(\frac{\eta_0}{6 \times 10^{-11}}\right)^{-\frac{1}{2}}$$
$$\text{for } \tau_x \gtrsim 3.8 \times 10^5 f^{-\frac{3}{2}} \text{sec}, \tag{5}$$

Here n_x/n_γ is the relic density (relative to blackbody photons) that the massive particle would have had today if it had not decayed.

Recently, Scherrer & Turner [19] have performed a detailed numerical study of this problem in which they adopt a realistic exponential distribution of decay times instead of assuming that all decays occur at $t = \tau_x$; this increases the change in η by $\sim 10\%$ over the estimate in eq. (1). By including the energy density of the massive particle and its decay products in the evolution equations without any approximations (*cf.* our assumption that $T_m \gg T_d$), they are able to consider earlier decay times. Their bound is shown as the full line in fig. 1, to be compared with the bound from eq. (5) shown as the dotted line; the two agree well when we note that they adopted a different lower bound, $\eta_0 \gtrsim 3 \times 10^{-11}$. They also study the effect on the D and ^3He abundances and impose the observationally-inferred constraint [11] $(D + {}^3He)/H < 10^{-4}$ (by number) to obtain a more restrictive bound shown as the dashed line in fig.

1. All these curves are drawn assuming $f_\gamma = 1$ and can be scaled for other values of f_γ (or η_0) using eq. (5). These bounds apply to any decaying particle which is non-relativistic during nucleosynthesis, *i.e.* with $m_x > \mathcal{O}(\text{MeV})$.

3 Bounds from the Effects of Decay Products on Elemental Abundances

We have considered above the effects of a massive decaying particle on nucleosynthesis through the change in the expansion rate and the entropy per nucleon. Far more stringent bounds obtain from consideration of the direct effects of the decay products on the synthesised elemental abundances.

For example, high energy photons or charged particles from a decaying particle initiate electromagnetic cascades in the radiation-dominated thermal background plasma, thus creating many low energy photons ($E_\gamma \approx 10$ MeV) capable of photodissociating the light elements [20]. Such photodissociations can occur only for $t \gtrsim 10^4$ sec, *i.e.* after nucleosynthesis is ***over***, since at earlier epochs the thermal photons are energetic enough and numerous enough that photon-photon interactions are far more probable than photon-nucleus interactions. When the x particle decays into energetic quarks or gluons, these fragment into hadronic showers which interact with the ambient nucleons thus changing their relative abundances [5]. If such hadronic decays occur *during* nucleosyntheis, the neutron-to-proton ratio is increased resulting in the production of more D and ^4He [25]. However when hadronic decays occur *after* nucleosynthesis, the result is destruction of ^4He and creation of D, ^3He, ^6Li and ^7Li [24].

When the x particle has both radiative and hadronic decay modes, the situation is then simplified by noting that for $\tau_x \sim 10^{-1} - 10^4$ sec, radiative decays do not play a significant role, whilst hadronic decays are constrained by the concommitant overproduction of D and ^4He by the hadronic showers [25]. For longer lifetimes, the situation is more complicated since elements may be simultaneously both created and destroyed by photo- and hadro- processes. It has been argued that, for $\tau_x \gtrsim 10^5$ sec, the most stringent bound on radiative decays comes from constraining the possible overproduction of D and ^3He through photodissociation of ^4He, since the simultaneous destruction of the former by photodissociation is negligible by comparison [18,26]. A somewhat weaker bound is obtained by constraining the depletion of the ^4He abundance itself [18,27]. These bounds are strengthened if hadronic decays also occur, since these too destroy ^4He and create D and ^3He. However, as we show below, these bounds are modified when the development of the electromagnetic cascades is studied taking $\gamma - \gamma$ scattering into account; this reveals that ^4He destruction is significant only for $\tau_x \gtrsim 5 \times 10^6$ sec, thus requiring correction of all previous work. It has also been argued that in the interval $\tau_x \sim 10^3 - 10^5$ sec, D is photodissociated but not ^4He, so that the strongest bound on radiative decays now

[5] The alteration of elemental abundances by direct annihilation with antinucleons has also been considered [21,22,23]; however this is not as important as the effect of the hadronic showers [24].

comes from requiring that D should not be excessively depleted [26,27]. Again, our reexamination of the cascade process indicates that the appropriate interval is shifted to $\tau_x \sim 5 \times 10^4 - 2 \times 10^6$ sec. This particular bound may appear to be circumvented if hadronic decay channels are also open since hadronic showers *create* D; however such showers also create the rare isotopes ^6Li and ^7Li, and are thus severely constrained by observational limits on their abundance [27]. This ensures that the D photofission bound is ***not*** affected by such hadronic decays.

We begin by reexamining the manner in which a massive particle decaying into photons or charged particles generates electromagnetic cascades in the radiation-dominated thermal plasma of the early Universe. The dominant mode of energy loss of a high energy photon (of energy E_γ) is e^+e^- pair production on the low energy thermal photons (of energy ϵ_γ) while the produced electrons and positrons lose energy by inverse-Compton scattering the thermal photons to high energies. Pair production requires $E_\gamma \epsilon_\gamma \geq m_e^2$, while $E_e \epsilon_\gamma \geq m_e^2$ implies that scattering occurs in the Klein-Nishina regime in which the electron loses a large fraction of its energy to the scattered photon. Thus a primary photon or electron triggers a cascade which develops until the photon energies have fallen below the pair-production threshold, $E_{max} = m_e^2/\epsilon_\gamma$. Subsequently the photons only undergo Compton scattering on the electrons and pair production on the ions of the thermal plasma. If the density of the thermal photons is large enough, the cascade is termed 'saturated', implying that nearly all of the primary particle energy is converted into photons with energy below E_{max}.

The spectrum of the 'breakout' photons below the pair-production threshold was originally found by Monte Carlo simulations of the cascade process to be [29,24]

$$\frac{dN}{dE_\gamma} \propto \begin{cases} E_\gamma^{-\frac{3}{2}} & \text{for } 0 \leq E_\gamma \leq E_{max} \equiv \frac{m_e^2}{\epsilon_\gamma}\,, \\ 0 & \text{for } E_\gamma > E_{max}\,, \end{cases} \tag{6}$$

when the background photons are assumed to be monoenergetic. Subsequently an analytic study of the kinetic equation for the cascade process showed that the spectrum actually steepens further to $\sim E_\gamma^{-1.8}$ for $E_\gamma \gtrsim 0.04\ E_{max}$ [30]. This feature had not been recognised in the Monte Carlo simulations due to insufficient statistics.

In the cosmological context, the background photons are not monoenergetic but have a Planck distribution at temperature T. We would naïvely expect that the pair-production threshold is then $E_{max} \sim m_e^2/T$ [18]. However, the primæval plasma is radiation-dominated, *i.e.* the number density of photons is very large compared to the number density of electrons and nuclei. Hence, even when the temperature is too low for a high-energy photon to pair-produce on the ***bulk*** of the thermal photons, pair-production may nevertheless occur on the photons in the Wien tail of the Planck distribution [20]. Although the spectrum here is falling exponentially with energy, the number of photons with $\epsilon_\gamma \gtrsim 25T$ is still comparable with the number of thermal electrons since $n_\gamma/n_e \gtrsim 10^9$. Therefore pair-production on such photons is as important as Compton scattering on electrons or pair-production on ions, the respective cross-sections being all comparable. Hence the value of E_{max} is significantly lowered below the above estimate, as seen by equating the mean free paths against

pair production on photons and Compton scattering on electrons [31]: [6]

$$E_{max} \simeq \frac{m_e^2}{20.4T[1 + \frac{1}{2}\ln(\frac{\eta}{7\times10^{-10}})^2 + \frac{1}{2}\ln(\frac{E_{max}}{m_e})^2]}\,. \tag{7}$$

Although various authors have previously noted this effect, they have used quite different estimates of E_{max}, for example $\sim m_e^2/12T$ [20,26], $\sim m_e^2/18T$ [28], $\sim m_e^2/25T$ [24,27] and $\sim m_e^2/32T$ [23]. Moreover, the spectrum has previously been assumed to be of the form (6) whereas for a blackbody target photon distribution it actually steepens to $\sim E_\gamma^{-1.8}$ for $E_\gamma \gtrsim 0.04 E_{max}$ [30].

None of the cited previous studies have included $\gamma - \gamma$ scattering. It was recently pointed out that this is, in fact, the *dominant* process in a radiation-dominated plasma for photons just below the pair-production threshold [31]. Therefore E_{max} should really be calculated as the energy for which the mean free paths against $\gamma - \gamma$ scattering and $\gamma - \gamma$ pair production are equal. For a Planck distribution of background photons this is

$$E_{max} \simeq \frac{m_e^2}{22T}\,; \tag{8}$$

photons pair-produce above this energy and scatter elastically below it. Another effect of $\gamma - \gamma$ scattering is reprocessing of the cascade spectrum leading to a further reduction in the number of high energy photons. The spectrum now falls like $\sim E_\gamma^{-1.5}$ up to the energy E_c where $\gamma - \gamma$ scattering and Compton scattering are equally probable, and then steepens to $\sim E_\gamma^{-5}$ before being cut off at E_{max} by the onset of pair production [30]. The value of E_c depends weakly on the photon energy; for the values relevant to photodissociation of light nuclei ($\sim 2.5 - 25$ MeV) we find it to be

$$E_c \simeq \left(\frac{m_e^2}{44T}\right)\left(\frac{\eta}{7\times10^{-10}}\right)^{\frac{1}{3}}\,, \tag{9}$$

i.e. effectively $E_c \simeq E_{max}/2$.

With this improved understanding of the cascade process we can now study how nuclear abundances are altered by photodissociation. Let dN_x/dE denote the spectrum of high-energy photons (or electrons) from massive particle decay, normalized as

$$\int_0^\infty E\frac{dN_x}{dE}dE = f_\gamma m_x\,, \tag{10}$$

where f_γ is the fraction of the x particle mass released in the form of electromagnetically interacting particles (easily calculable once the decay modes and branching ratios are specified). A decay photon (or electron) of energy E initiates a cascade with the spectrum

$$\frac{dn_E}{dE_\gamma} = \begin{cases} \frac{24\sqrt{2}}{55}\frac{E}{\sqrt{E_{max}}}E_\gamma^{-\frac{3}{2}} & \text{for } 0 \leq E_\gamma \leq E_{max}/2, \\ \frac{3}{55}EE_{max}^3E_\gamma^{-5} & \text{for } E_{max}/2 \leq E_\gamma \leq E_{max}, \\ 0 & \text{for } E_\gamma > E_{max}, \end{cases} \tag{11}$$

[6] At the energies relevant to photodissociation processes ($E_\gamma < 100$ MeV), pair-production on ions is unimportant by comparison with Compton scattering [31].

where the cascade spectrum has been normalised as

$$\int_0^{E_{max}} E_\gamma \left(\frac{dn_E}{dE_\gamma}\right) dE_\gamma = E\,, \qquad E_{max} = \frac{m_e^2}{22T}\,. \tag{12}$$

The balance equation for the change in the abundance of element i with total photodissociation cross-section σ_i (above threshold Q_i) is [18] [7]

$$\frac{dX_i}{dt}|_{photo} = -\frac{dn_x}{dt}\int_0^\infty \frac{dN_x}{dE}dE\left[\int_{Q_i}^E \frac{dn_E}{dE_\gamma}\frac{X_i\sigma_i}{n_e\sigma_C}dE_\gamma - \sum_{j\neq i}\int_{Q_i}^E \frac{dn_E}{dE_\gamma}\frac{X_j\sigma_{j\to i}}{n_e\sigma_C}dE_\gamma\right], \tag{13}$$

where $\sigma_{j\to i}$ is the partial cross-section for photodissociation of element i to element j, and σ_C is the cross-section for Compton scattering on the thermal electrons of density

$$n_e \simeq \frac{7}{8}n_N = \frac{7}{8}\eta n_\gamma\,, \tag{14}$$

for a $H + He$ plasma with $He/H \simeq 0.1$ [8]. Since the number density of x particles decreases from its initial value n_x^0 as

$$\frac{dn_x}{dt} = -\frac{n_x^0}{\tau_x}\exp\left(-\frac{t}{\tau_x}\right), \tag{15}$$

the time-integrated change in the elemental abundance (in a comoving volume) is given by

$$\begin{aligned}
\int_{t_i^{min}}^\infty \frac{dX_i}{dt}|_{photo}\,dt &\simeq \left(m_x\frac{n_x}{n_\gamma}\right)\frac{f_\gamma}{\eta}\left[-X_i\beta_i(\tau_x) + \sum_{j\neq i}X_j\beta_{j\to i}(\tau_x)\right], \\
\beta_i(\tau_x) &\equiv \int_{t_i^{min}}^\infty dt\exp\left(-\frac{t}{\tau_x}\right)\int_{Q_i}^{E_{max}(t)}\left(\frac{1}{E}\frac{dn_E}{dE_\gamma}\right)\frac{\sigma_i(E_\gamma)}{\sigma_c(E_\gamma)}dE_\gamma\,, \\
\beta_{j\to i}(\tau_x) &\equiv \int_{t_j^{min}}^\infty dt\exp\left(-\frac{t}{\tau_x}\right)\int_{Q_j}^{E_{max}(t)}\left(\frac{1}{E}\frac{dn_E}{dE_\gamma}\right)\frac{\sigma_{j\to i}(E_\gamma)}{\sigma_c(E_\gamma)}dE_\gamma\,,
\end{aligned} \tag{16}$$

(We have dropped the superscript ^{0} on n_x above and hereafter.)

The time t_i^{min} at which photodissociation of element i starts is computed from the time-temperature relationship for a radiation-dominated Universe,

$$t \simeq 1.66 g_*^{-\frac{1}{2}}\frac{T^2}{M_P} \tag{17}$$

(with $g_* \simeq 3.36$ for $T \ll m_e$), corresponding to the critical temperature at which the cascade cutoff energy E_{max} equals the photodissociation threshold Q_i.

The integrals for β_i and $\beta_{j\to i}$ were computed numerically for various values of τ_x using the cascade spectrum of eq. (11) and the cross-sections referenced in earlier

[7] Recombination of the dissociated nuclei, in particular D, is negligible for $t \gtrsim 10^4$ sec.

[8] Anticipating the stringent constraints to be derived shortly, we can assume that η is not altered significantly by the particle decays.

work [18,24]. As seen in fig. 2, β rises sharply from zero above a critical value of τ_x (which increases as the square of the photodissociation threhold), peaks at a value which is nearly the same (≈ 1 GeV^{-1}) for all light elements, and subsequently falls off rather slowly with increasing τ_x. This reflects the fact that the relevant photodissociation cross-sections are all of order a few millibarns above threshold and fall rapidly thereafter with increasing energy. Photodissociation begins when the cascade cutoff energy just crosses the photodissociation threshold, and the dominant effect is that of photons with energies just over this threshold.

This implies that when photodissociation of ^4He occurs, the resultant production of D and ^3He ($\gamma\,^4He \to n\,^3He$, $p\,^3H$, $p\,n\,D$; $^3H \to {}^3He\,e^-\,\bar{\nu}_e$) far dominates their destruction since the abundance of ^4He is $\sim 10^4$ times greater [18]. As seen in fig. 2, photodissociation of D begins at $\tau_x \sim 10^4$ sec and becomes significant at $\tau_x \sim 10^5$ sec, whilst photodissociation of ^4He begins at $\tau_x \sim 10^6$ sec and becomes significant at $\tau_x \sim 10^7$ sec. Therefore for $\tau_x \gtrsim 10^6$ sec we can simplify eq. (16) to read, for the difference between the initial and final mass fractions of $D + {}^3He$

$$X_f(D+{}^3He) - X_i(D+{}^3He) \simeq Y_i({}^4He)\left(m_x\frac{n_x}{n_\gamma}\right)\frac{f_\gamma}{\eta}r\beta_{^4He}(\tau_x), \tag{18}$$

where $r \equiv (\frac{3}{4}\sigma_{\gamma\,^4He\to n\,^3He,p\,^3H} + \frac{1}{2}\sigma_{\gamma\,^4He\to p\,n\,D})/\sigma_{\gamma\,^4He\to all} \simeq 0.5$, and the subscripts i and f refer to initial and final values. To obtain the most conservative bound on the decaying particle we must consider the maximum value allowed for $[X_f(D + {}^3He) - X_i(D + {}^3He)]\,\eta/Y_i({}^4He)$. Since ^4He cannot have been destroyed significantly (without overproducing D and ^3He) we take its initial abundance to be the maximum permitted, *i.e.* $Y_i(^4He) < 0.25$ [3]. This implies that $\eta < 1.3 \times 10^{-9}$, adopting the recently revised neutron lifetime and allowing for 2σ uncertainties in all relevant nuclear reaction rates [33]. Hence a minimum mass fraction $X_i(D + {}^3He) > 3.4 \times 10^{-5}$ would have been primordially synthesised. The maximum final abundance after photoproduction, consistent with 'standard' galactic chemical evolution, is bounded by $(D + {}^3He)/H < 10^{-4}$ by number, *i.e.* $X_f(D + {}^3He) \lesssim 2.3 \times 10^{-4}$ [11]. Using these numbers and taking $f_\gamma = 1$ yields the upper bound on $m_x n_x/n_\gamma$ shown in fig. 3 above which $D + {}^3He$ is overproduced. For reference the dashed line indicates the bound obtained by Ellis, Nanopoulos & Sarkar [18] using the same argument but with a less sophisticated treatment of the cascade process. A similar bound was obtained by Juszkiewicz, Silk & Stebbins [26]. We cannot reproduce the (less stringent) bound quoted by Kawasaki & Sato [28] even after adopting their (incorrect) cascade spectrum; since their result was obtained entirely from a computer code, the reason for the discrepancy cannot be easily traced. Dimopoulos *et al* [27] chose not to consider the bound on the decaying particle abundance from photoproduction of $D + {}^3He$. These authors criticise Ellis *et al* [18] for having neglected the photodissociation of D by comparison, but as shown above this is quite justified since the correction is only $\mathcal{O}(10^{-4})$.

For $\tau \lesssim 10^6$ sec, photodissociation of ^4He is not significant so D and ^3He are not produced but only destroyed. Assuming that hadronic decay channels are not open,

eq. (16) now reads for the change in the D mass fraction alone

$$\frac{X_i(D)}{X_f(D)} \simeq \exp\left[\left(\frac{m_x n_x}{n_\gamma}\right)\frac{f_\gamma}{\eta}\beta_D(\tau_x)\right] \tag{19}$$

Again, to obtain the most conservative bound on the particle abundance, we must consider the maximum extent to which D may have been depleted. Given the bound $\eta > 10^{-10}$ corresponding to the observational constraint $Y_p(^4He) > 0.22$, [3] the primordially synthesised D mass fraction is bounded by $X_i(D) < 10^{-3}$. The minimum final abundance after photodissociation is observationally bounded by $D/H > 10^{-5}$ (by number), *i.e.* $X_f(D) > 2 \times 10^{-5}$ [11]. This gives $\eta \ln[X_i(D)/X_f(D)]$ to be $\sim 4 \times 10^{-10}$, but in fact we can increase it further to $\sim 6 \times 10^{-10}$ by choosing a higher value of η and a correspondingly lower value of $X_i(D)$. The corresponding upper bound on the decaying particle abundance is indicated in fig. 3 above which D is excessively depleted. The dotted line alongside is the bound obtained by Dimopoulos *et al* [27] from similar considerations but ignoring $\gamma - \gamma$ scattering. All the above bounds apply to any decaying particle which can generate electromagnetic cascades above the photodissociation threholds; this requires $m_x \gtrsim 10 - 50$ MeV depending on which element is being considered.

As mentioned earlier, when hadronic decay channels are open, D is *produced* by hadronic showers and this requires reconsideration of the bound derived above. In fact, even if the particle decays exclusively into photons, the resulting electromagnetic cascades will be effectively hadronic for $E_\gamma \epsilon_\gamma > \mathcal{O}(\mathrm{GeV}^2)$. Furthermore, there is always a $\sim 1\%$ probability for the (virtual) decay photon to convert into a $q\bar{q}$ pair over threshold. Hence hadronic showers will be generated if the particle is sufficiently massive ($m_x > \mathcal{O}(\mathrm{GeV})$) even if it has no specific hadronic decay channels [25].

As discussed in detail by Dimopoulos *et al* [24,27], the main effect of hadronic showers is the destruction of the ambient ^4He nuclei and the creation of D, ^3He, ^6Li and ^7Li. The average number of i nuclei created per x particle decay, ξ_i, can be computed by modelling the hadronic shower development using e^+e^- jet data. The balance equation (13) is now modified to read

$$\frac{dX_i}{dt} = \frac{dX_i}{dt}|_{photo} + \frac{dX_i}{dt}|_{hadro}\,, \tag{20}$$

where the first term is as before and the second term is [24]

$$\frac{dX_i}{dt}|_{hadro} = r_B^* \xi_i \frac{dn_x}{dt}\,, \qquad r_B^* \equiv \left(\frac{\nu_B}{5}\right) r_B \mathcal{F}\,. \tag{21}$$

Here r_B^* is an 'effective' baryonic branching ratio defined in terms of the true baryonic branching ratio r_B, the baryonic multiplicity ν_B, and a factor $\mathcal{F}$ representing the dependence of the yields ξ_i on the energy of the primary shower baryons. The e^+e^- jet production data suggest that for $m_x = 1$ TeV, there are ~ 5 nucleon-antinucleon pairs produced with ~ 5 GeV energy/nucleon. For other values of m_x, ν_B depends logarithmically on the energy, except near the baryon production threshold where the dependence is somewhat stronger.

Considering the effects of hadroproduction alone, eq. (21) integrates to read [27]

$$\frac{n_x^0}{n_\gamma} < \frac{(\mathcal{N}_i^{max} - \mathcal{N}_i^{min})\eta}{r_B^* \xi_i}\,, \tag{22}$$

where $\mathcal{N}_i^{max}$ and $\mathcal{N}_i^{min}$ are, respectively, the maximum (observed) and minimum (synthesised) abundance of element i ***by number***, relative to hydrogen. This constraint can be imposed on the hadroproduction of D, ^3He, ^6Li and ^7Li. Taking $\mathcal{N}_{^7Li}^{max} \sim 2 \times 10^{-10}$ and $\mathcal{N}_{^7Li}^{min} \sim 5 \times 10^{-11}$, this gives [27]

$$\frac{n_x^0}{n_\gamma} < 1.5 \times 10^{-5} \frac{\eta}{r_B^*}\,. \tag{23}$$

A similar bound follows from requiring $\mathcal{N}_{(D+^3He)}^{max} \sim 10^{-4}$. An even stricter bound can be obtained if one assumes that the primordial abundance of ^6Li did not exceed its presently observed value, *i.e.* $\mathcal{N}_{^6Li}^{max} \sim 10^{-11}$. This yields [27]

$$\frac{n_x^0}{n_\gamma} < 3 \times 10^{-7} \frac{\eta}{r_B^*}\,. \tag{24}$$

The fact that these bounds are so very restrictive considerably simplifies the situation when *both* electromagnetic and hadronic showers occur. For a given x particle abundance, the hadronic branching ratio must be very small in order not to overproduce Li. This ensures that the production of D by hadronic showers is quite negligible relative to its production by electromagnetic showers. This is borne out by numerical solution of eq. (20) taking both kinds of showers into account [27]. It is true that in a small region of parameter space ($\tau_x \approx 10^5 - 10^6$ sec, $m_x n_x/n_N \approx 10^1 - 10^3$ GeV, $r_B^* n_x/n_N \approx 10^{-4} - 10^{-2}$), the upper bound on the decaying particle abundance from the photodissociation of D *is* evaded by compensatory hadroproduction of D. However, the required values of $r_B^* n_x/n_N$ would result in overproduction of ^7Li and ^6Li (see eqs. (23), (24)). Furthermore, the values required for $m_x n_x/n_N$ may cause an observable distortion of the blackbody spectrum of the relic photons (see §4). Therefore the bounds derived from consideration of photodissociation processes are *not* evaded even if hadronic decay channels are also open.

For $\tau_x < 10^4$ sec, photodissociation does not occur for any element and standard nucleosynthesis is unaffected by electromagnetic showers. However, hadronic showers can induce interconversions between the ambient protons and neutrons, thus changing the equilibrium n/p ratio. This has been studied in detail by Reno & Seckel [25]; we summarise their analysis below in order to make use of their results.

The transition rate for a thermal nucleon to convert to another nucleon is the usual weak interaction rate plus the rate due to hadronic showers, given by [25]

$$\Gamma_{p\to n} = \frac{\Gamma_x n_x}{X(p) n_N} \sum \mathcal{P}_{x_i} f_{pn}^i\,, \qquad \Gamma_{n\to p} = \frac{\Gamma_x n_x}{X(n) n_N} \sum \mathcal{P}_{x_i} f_{np}^i\,, \tag{25}$$

where $\Gamma_x \equiv \tau_x^{-1}$, $X(p)$ and $X(n)$ are the proton and neutron fractions, $\mathcal{P}_{x_i}$ is the average number of hadronic species i per x particle decay and f_{pn}^i, f_{np}^i are the probabilities for i to induce the respective transitions. The fragmentation process can be

modelled using data on jet multiplicities from e^+e^- annihilation experiments [25]:

$$\mathcal{P}_{x_i} \simeq N_{jet}\langle n_{ch}(E_{jet})\rangle B_h \left(\frac{n_i}{n_{ch}}\right). \tag{26}$$

Here B_h is the hadronic branching ratio for x decay, N_{jet} is the number of jets, and n_i, the charge multiplicity of species i, has been expressed as a fraction of the average charge multiplicity $\langle n_{ch}(E_{jet})\rangle$ at a given energy E_{jet}. The transition probability is computed as the ratio of the strong interaction rate to the sum of the decay and absorption rates for the injected hadrons:

$$f^i_{pn} = \frac{\Gamma^i_{pn}}{\Gamma^i_D + \Gamma^i_A}, \qquad f^i_{np} = \frac{\Gamma^i_{np}}{\Gamma^i_D + \Gamma^i_A}. \tag{27}$$

When the decaying particle carries no baryon number, the decay hadrons can be thought of as being injected in pairs so that i can refer to mesons as well as to baryon-antibaryon pairs (*i.e.* $i = n\bar{n}, p\bar{p}, \ldots$). The injected hadrons are stopped (except K_L) before they interact with the ambient neutrons so that threhold values of cross-sections can be used [25]. The variable quantifying the effect of hadronic decays is then the x particle abundance multiplied by a parameter F defined as

$$F \equiv \frac{N_{jet}B_h}{2}\frac{\langle n(E_{jet})\rangle}{\langle n(E \simeq 33\ \mathrm{GeV})\rangle}, \tag{28}$$

so that $F \simeq 1$ for $m_x = 100$ GeV, if we take $E_{jet} \simeq m_x/3$, $n_{jet}B_h = 2$, *i.e.* assuming that x decays into 3 particles at the parton level (e.g. gravitino $\tilde{G} \to q\bar{q}\gamma$) and N_{jet} equals the number of (non-spectator) quarks at the parton level.

The neutron fraction in the thermal plasma is always less than 0.5, being 0.16 at $T \simeq 0.7$ MeV when the weak interaction rate falls behind the expansion rate, and decreasing (by beta decay) to 0.12 at $T \simeq 0.09$ MeV where the 'deuterium bottleneck' breaks and nuclear reactions begin. Since there are always more protons than neutrons, the overall effect of hadronic decays in the interval $\tau_x \sim 1 - 100$ sec is to convert protons into neutrons. (For injection of $p\bar{p}$ pairs, the neutron fraction is actually reduced but this is compensated for by the effects of mesons and $n\bar{n}$ injection.) The additional neutrons thus produced are all synthesised into ^4He and hence hadronic decays in this lifetime interval are constrained by the observational upper bound to the helium abundance.

Reno & Seckel [25] obtain bounds on Fn_x/n_γ as a function of τ_x for $\eta = 3 \times 10^{-10}$ and 10^{-9}, adopting the constraint $Y_p(^4He) < 0.26$. We have rescaled their results (for the case when x does not itself carry baryon number) to the more stringent constraint $Y_p(^4He) < 0.25$; [3] this requires that we restrict ourselves to the case $\eta = 3 \times 10^{-10}$ (since for $\eta = 10^{-9}$, Y_p already exceeds 0.25 even in the absence of x decays). We calculate the resulting upper bound on $m_x n_x/n_\gamma$ taking $B_h = 1$ (the bound scales inversely as B_h) and show this in fig. 3. The bound gets more stringent as τ_x increases from 0.1 sec to 100 sec since the neutron fraction is dropping in this time interval. At later times the neutron fraction is effectively zero (since all neutrons are now bound in nuclei) and the only free neutrons are those created by x decay. These additional neutrons can bind into D but D cannot burn further to ^4He since

the corresponding reaction rate is now too low due to the falling number densities. For $\tau_x \sim 100 - 1000$ sec, the ^3He abundance is also increased by $D - D$ burning. For $\tau_x \gtrsim 10^4$ sec the released neutrons decay before forming D. Hence in the interval $10^2 - 10^4$ sec, the appropriate constraint on hadronic decays is the observationally inferred bound $(D +^3 He)/H < 10^{-4}$ (by number) [11]. The corresponding upper bound on $m_x n_x/n_\gamma$, extracted from ref. [25], is also shown in fig. 3.

The results presented above constitute the most stringent bounds on massive particle decays in the early Universe, imposed by the success of the standard Big Bang nucleosynthesis model in matching the observationally inferred abundances.

4 Bounds from the 2.7 ^{0}K Background Radiation

Recent observations [34] by the *COBE* satellite have decisively demonstrated that the cosmic microwave background radiation has the spectrum of a blackbody with temperature

$$T_0 = 2.735 \pm 0.06\,^0\mathrm{K}, \tag{29}$$

in the range $\lambda \sim 0.05 - 1$ cm. A balloon-borne experiment [35] has provided further confirmation in the range $\lambda \sim 0.06 - 0.3$ cm; these authors find

$$T_0 = 2.736 \pm 0.017\,^0\mathrm{K}, \tag{30}$$

Together with previous ground-based observations at longer wavelengths [36], these results severely constrain spectral distortions which may been induced by the radiative decays of massive relic particles [18,26].

To quantify this, it is necessary to study how scattering processes in the early Universe establish a Planck spectrum for the relic photons [37]. The evolution equation for the photon occupation number is

$$\frac{\partial \eta}{\partial t} = \frac{\partial \eta}{\partial t}|_C + \frac{\partial \eta}{\partial t}|_B + \frac{\partial \eta}{\partial t}|_{DC}\,. \tag{31}$$

Here the first term on the right-hand side describes the Compton scattering of low-energy ($\epsilon_\gamma \ll m_e$) photons with a thermal Maxwellian electron plasma at temperature $T_e \ll m_e$:

$$\frac{\partial \eta}{\partial t}|_C = \frac{1}{t_{\gamma e}}\frac{T_e}{m_e}\frac{1}{x^2}\frac{\partial}{\partial x}\left[x^4\left(\frac{\partial \eta}{\partial x} + \eta + \eta^2\right)\right], \quad x \equiv \frac{\epsilon_\gamma}{T_e}, \tag{32}$$

where

$$t_{\gamma e} = \frac{1}{(n_e \sigma_T)} \simeq 6.4 \times 10^{-11}\ \mathrm{sec}\left(\frac{T}{\mathrm{MeV}}\right)^{-3}\frac{\Theta^3_{2.7}}{\Omega_N h^2},$$
$$\Theta_{2.7} \equiv \frac{T_0}{2.7\,^0\mathrm{K}}, \tag{33}$$

is the time-scale for Thomson scattering (taking $n_e \sim 0.9 n_N$ for a H + He plasma with $n_{He}/n_H \sim 0.1$). This describes the diffusion of photons in energy space, with

the photon energy increasing on average per collision by $\langle \Delta\nu/\nu \rangle \sim T_e/m_e$ due to the Doppler effect. The most general equilibrium solution, for which $(\partial\eta/\partial x)+\eta+\eta^2 = 0$, is of the Bose-Einstein form

$$\eta_{BE} = \frac{1}{(e^{x+\mu}-1)}, \tag{34}$$

where μ is a dimensionless chemical potential. This spectrum is established on the 'Comptonization' time scale

$$t_C = \left(\frac{m_e}{T_e}\right) t_{\gamma e} \simeq 3.3 \times 10^{-11} \text{ sec} \left(\frac{T}{\text{MeV}}\right)^{-4} \left(\frac{T}{T_e}\right) \Omega_N h^2 \Theta_{2.7}^3. \tag{35}$$

Radiation at temperature T, in *chemical* equilibrium with the thermal plasma, would have $\mu = 0$, *i.e.* the Planck spectrum

$$\eta_{Pl} = \frac{1}{(e^x - 1)}, \quad T_e = T. \tag{36}$$

However, since Compton scattering conserves photon number, it cannot create a Planck spectrum if, say, the initial spectrum has *fewer* photons than a blackbody of the same total energy; in this case $\mu > 0$. To establish a Planck spectrum requires the generation of new photons by radiative processes such as bremsstrahlung ($e + ion \rightarrow e + ion + \gamma$) and double Compton scattering ($e + \gamma \rightarrow e + \gamma + \gamma'$). Their rates are [38], for bremsstahlung,

$$\begin{aligned}
\frac{\partial\eta}{\partial t}|_B &= \frac{1}{t_{\gamma e}} \left[\frac{Qg(x)}{e^x}\right] \frac{1}{x^3} \left[1 - \eta(e^x - 1)\right], \\
Q &= \frac{1}{\sqrt{2\pi}} \left(\frac{m_e}{T_e}\right)^{\frac{1}{2}} \alpha \left(\sum n_i Z_i^2\right) T_e^{-3} \\
&\simeq 1.4 \times 10^{-11} \left(\frac{T}{\text{MeV}}\right)^{-\frac{1}{2}} \left(\frac{T}{T_e}\right)^{\frac{7}{2}} \frac{\Omega_N h^2}{\Theta_{2.7}^3}, \\
g(x) &= \begin{cases} \ln\left(\frac{2.25}{x}\right) & \text{for } x \lesssim 1 \\ \frac{\ln 2.25}{\sqrt{x}} & \text{for } x \gtrsim 1, \end{cases}
\end{aligned} \tag{37}$$

and, for double Compton scattering,

$$\begin{aligned}
\frac{\partial\eta}{\partial t}|_{DC} &= \frac{1}{t_{\gamma e}} \left[\frac{4\alpha}{3\pi} \left(\frac{T_e}{m_e}\right)^2 I(t)\right] \frac{1}{x^3} \left[1 - \eta(e^x - 1)\right], \\
I(t) &= \int x^4 (1+\eta)\, \eta\, dx.
\end{aligned} \tag{38}$$

In eq. (38), $g(x)$ is the Gaunt factor and n_i the ion density ($n_i Z_i^2 = n_N$ for a H + He plasma). Note that both rates have three terms, corresponding respectively to spontaneous emission, absorption and stimulated emission, and that both rates vanish for $\eta = \eta_{Pl}$. This ensures that the equilibrium solution to the full evolution equation (31) is indeed the Planck spectrum, which is reached by a three-stage process. Radiative processes create mainly soft photons which are then scattered up in energy on the (energy-independent) Comptonization time scale t_C [eq. (35)]. As the number

density of photons approaches that of a Planck distribution, photon *absorption* by radiative processes becomes important and the spectrum relaxes to the Planck shape. This is first achieved at low energies where the new photons are absorbed before they can be scattered up. At high energies photons are more likely to be scattered than absorbed, hence it takes longer for the Planck shape to be established here.

In the early Universe at sufficiently high temperatures, rapid particle-antiparticle pair annihilations ensure that the photons are in chemical equilibrium and have the Planck spectrum. Even after all pairs have annihilated (*i.e.* for $T \lesssim m_e$) radiative scattering processes can generate photons sufficiently rapidly down to a critical thermalisation redshift z_{Pl} (to be derived shortly) such that a Planck spectrum is promptly restored following any attempt at distortion. Hence dissipative processes can make a mark on the photon spectrum only if they occur at $z < z_{Pl}$; conversely an arbitrarily large energy release is allowed only for $z > z_{Pl}$.

Now consider the decay of an unstable particle into photons or charged particles which ultimately releases (through electromagnetic cascades) an arbitrary spectrum of photons of total energy $\Delta\rho_\gamma$ and number Δn_γ into the thermal bath of blackbody radiation and plasma at a (common) temperature T. The non-thermal photons Compton scatter against and heat the electrons in the plasma, which then heat the thermal photons through inverse Compton scattering. (Direct photon-photon scattering has a negligible cross-section unless the product of photon energies exceeds m_e^2.) The net result is the creation of a Bose-Einstein spectrum, with energy density

$$\begin{aligned}
\rho_{BE} &= \rho_\gamma + \Delta\rho_\gamma \equiv \frac{\pi^2}{15} T_e^4\, f(\mu), \\
f(\mu) &= \frac{15}{\pi^4} \int \frac{x^3}{(e^{x+\mu}-1)} dx \simeq \begin{cases} \frac{90}{\pi^4} e^{-\mu} & \text{for } \mu \gg 1, \\ 1 - \frac{90\zeta(3)}{\pi^4}\mu & \text{for } \mu \ll 1, \end{cases}
\end{aligned} \tag{39}$$

and number density

$$\begin{aligned}
n_{BE} &= n_\gamma + \Delta n_\gamma \equiv \frac{2\zeta(3)}{\pi^2} T_e^3\, \phi(\mu), \\
\phi(\mu) &= \frac{1}{2\zeta(3)} \int \frac{x^2}{(e^{x+\mu}-1)} dx \simeq \begin{cases} \frac{e^{-\mu}}{\zeta(3)} & \text{for } \mu \gg 1, \\ 1 - \frac{\pi^4}{\zeta(3)}\mu & \text{for } \mu \ll 1. \end{cases}
\end{aligned} \tag{40}$$

Here $f(\mu)$ and $\phi(\mu)$ express the deviation in energy density and number density, respectively, from a Planck spectrum at the same temperature.

When the decaying particle is non-relativistic, its number density is much smaller than that of the thermal photons and hence the number of decay photons is also small (even taking cascade secondaries into account):

$$\Delta n_\gamma \ll n_\gamma = \frac{2\zeta(3)}{\pi^2} T^3, \tag{41}$$

Hence initially the electrons are heated to a temperature [9]

$$T_e \simeq \frac{T}{[\phi(\mu_0)]^{\frac{1}{3}}}, \tag{42}$$

[9] The redshifting of the photons can be ignored since the thermalisation time is much shorter than the expansion time scale.

and the initial chemical potential μ_0 is therefore related to the energy release as

$$\frac{\Delta\rho_\gamma}{\rho_\gamma} = \frac{f(\mu_0)}{[\phi(\mu_0)]^{\frac{4}{3}}} - 1 \simeq \begin{cases} 1.18\, e^{\frac{\mu_0}{3}} - 1 & \text{for } \mu_0 \gg 1, \\ 0.714\,\mu_0 & \text{for } \mu_0 \ll 1. \end{cases} \tag{43}$$

As discussed earlier, radiative processes rapidly reduce μ to zero when the distortion is induced above a critical redshift z_{PI}. The dominant radiative process at high redshifts ($z \gtrsim 10^7$) is double-Compton scattering since bremsstrahlung is not as efficient in a low nucleon density Universe (which is required by primordial nucleosynthesis arguments). In this case the photon number increases exponentially on the time scale [38]

$$\begin{aligned} t_{DC} &= \frac{\pi}{8\alpha}\left(\frac{m_e}{T_e}\right)^2 t_{\gamma e} \\ &\simeq 9.0 \times 10^{-10}\ \text{sec}\ \left(\frac{T}{\text{MeV}}\right)^{-5}\left(\frac{T}{T_e}\right)^2 \frac{\Theta_{2.7}^3}{\Omega_{N_0} h^2}. \end{aligned} \tag{44}$$

Although this time-scale was derived [38] for the case of an isothermal plasma, numerical integration of the governing equations shows [16] that it is also applicable to the case at hand if the energy release by the decaying particle is large, *i.e* for $\mu_0 \gg 1$. The critical redshift z_{PI} (corresponding to the epoch t_{PI}) is then given by the condition

$$\int_0^{t_{PI}} \frac{dt}{t_{DC}} \simeq 1 \tag{45}$$

to be [16]

$$z_{PI} \simeq \frac{3.9 \times 10^6}{(\Omega_N h^2)^{\frac{1}{3}}} \qquad \text{for } \mu \gg 1. \tag{46}$$

At $z < z_{PI}$ the primary operative process is Compton scattering. The change this induces in the photon energy is measured by the parameter

$$y = -\int_0^{t(z)} \frac{dt}{t_C}, \tag{47}$$

which becomes less than unity when the redshift falls below a critical value [37]

$$z_{BE} \simeq \frac{1.9 \times 10^4}{(\Omega_N h^2)^{\frac{1}{2}}}. \tag{48}$$

Hence any energy release at $z > z_{BE}$ will be thermalised sufficiently to form a Bose-Einstein spectrum but radiative processes are no longer efficient enough at $z < z_{PI}$ to reduce μ to zero. Since the spectrum is, in fact, observed to be Planckian within the experimental uncertainties, such a chemical potential is bounded by $\mu_0 < 8 \times 10^{-3}$ at 95% c.l. [34,35]. Using eq. (43) this translates into the constraint

$$\frac{\Delta\rho_\gamma}{\rho_\gamma} < 5.7 \times 10^{-3}, \tag{49}$$

on any non-thermal energy release in the interval $z_{BE} < z < z_{PI}$.

In fact this bound is overly restrictive in the neighbourhood of z_{PI} since photon creation by double Compton scattering does occur to some extent even for $z \lesssim z_{PI}$, thus reducing μ below μ_0. The relaxation of the bound on the decaying particle energy density as z approaches z_{PI} from below can be studied by numerical integration of the governing equations. This has been done by Juszkiewicz, Silk and Stebbins [26] in order to obtain the abundance of massive decaying gravitinos which yield final values for μ of 10^{-2} and 10^{-3}. Using these results and interpolating appropriately, we have extracted bounds on $\Delta\rho_\gamma/\rho_\gamma$, applicable to any decaying particle, which respect the observational limit (49). (A more detailed numerical study of this problem is in progress [39].)

Energy release at $z < z_{BE}$ will not be thermalised at all but simply heat the electrons to a temperature $T_e > T$. Inverse-Compton scattering will then create a distorted spectrum characterised by the parameter

$$u = \int_0^{t(z)} \left(1 - \frac{T_e}{T}\right) \frac{dt}{t_c}. \tag{50}$$

which is related to the energy release in non-thermal photons as

$$\frac{\Delta\rho_\gamma}{\rho_\gamma} = e^{4u} - 1 \simeq 4u \qquad \text{for } u \ll 1. \tag{51}$$

The distorted spectrum can now be represented by a linear superposition of Planck spectra. Since scattering conserves the total photon number while increasing the average photon energy, the brightness temperature will be depressed in the Rayleigh-Jeans region and increase sharply at the Wien end. An earlier claim by a rocket-borne experiment [40] for just such a distortion is refuted by the new data which sets the upper limit $u < 10^{-3}$ at 95% c.l. [34,35], implying the following constraint on any energy release at $z < z_{BE}$,

$$\frac{\Delta\rho_\gamma}{\rho_\gamma} < 4 \times 10^{-3}. \tag{52}$$

This bound nominally applies down to the (re)combination epoch $z_{rec} \sim 1100$ when the photons decouple from the plasma. Any subsequent energy release cannot create spectral distortions unless the Universe is reionized allowing Compton scattering to provide again the necessary coupling. The same constraint would then apply to that part of the released energy which is communicated to the relic photons. However, for $z \lesssim 4$ (corresponding to $t \gtrsim 10^9$ yr), the electron cooling time-scale $t_{e\gamma} = (3m_e/4\sigma_T\rho_\gamma) \simeq 2.3 \times 10^{-19}\ \text{sec}\ (T/MeV)^{-4}$ exceeds the expansion age, hence only a small fraction of any energy release can be transferred to the thermal photons.

The above bounds can be translated into bounds on the energy density (as a function of the lifetime) of any decaying non-relativistic particle. Since the energy release is constrained to be small, the mass density of the decaying particle could not have perturbed the expansion rate significantly (unless the radiative branching ratio is very small). Hence the cosmological epochs t_{rec} and t_{BE} corresponding to the redshifts z_{rec} and z_{BE} can be simply computed from the canonical time-temperature relationship, taking matter domination to occur at $z_m \simeq 2.5 \times 10^4\,(\Omega h^2 \Theta_{2.7}^{-4})$. However, the thermalisation redshift z_{PI} is derived for the case of an arbitrarily large energy

release, hence the heavy particle may well have itself matter-dominated the expansion before decaying. Therefore the value of t_{Pl} which is calculated below assuming the usual radiation-dominated Universe should be regarded as an upper limit.

The resulting constraints on any radiatively decaying particle of mass $> \mathcal{O}$ (MeV) are

$$\begin{aligned}
\left(\frac{m_x}{\mathrm{GeV}}\right)\left(\frac{n_x}{n_\gamma}\right) &\lesssim 1.8\times 10^{-5}\left(\frac{\tau_x}{\mathrm{sec}}\right)^{-\frac{1}{2}} f_\gamma^{-1} \\
\text{for } t_{BE} &\sim 6.5\times 10^{8}\left(\frac{\Omega_N h^2}{0.01}\right)\Theta_{2.7}^{-2} \gtrsim \left(\frac{\tau_x}{\mathrm{sec}}\right) \gtrsim t_{Pl} \sim 7.4\times 10^{4}\left(\frac{\Omega_N h^2}{0.01}\right)^{\frac{2}{3}}\Theta_{2.7}^{-2}, \\
&\lesssim 1.2\times 10^{-5}\left(\frac{\tau_x}{\mathrm{sec}}\right)^{-\frac{1}{2}} f_\gamma^{-1} \\
\text{for } t_{rec} &\sim 5.4\times 10^{12}(\Omega h^2)^{-\frac{1}{2}} \gtrsim \left(\frac{\tau_x}{\mathrm{sec}}\right) \gtrsim t_{BE}\,. \qquad (53)
\end{aligned}$$

These are shown in fig. 4, with the relaxation of the bound as t approaches t_{Pl} indicated by the dotted line.

While these bounds are not as stringent as those derived from primordial nucleosynthesis arguments, they are arguably more reliable. This is because the relic photon spectrum is *directly* observable, while the primordial elemental abundances have to be *inferred* from their present values using astrophysical arguments.

5 Bounds from the Gamma-ray Background

As noted in the previous section, radiative decays which occur after (re)combination cannot distort the 2.7 ^{0}K background; however, the non-thermal decay photons may be directly visible today if the optical depth back to the decay epoch is small enough. The diffuse extragalactic γ-ray background radiation observed in the range $\sim 0.3-200$ MeV [41] can be compared to the expected flux and upper bounds can thereby be extracted on the decaying particle abundance.

Fortunately, the universe is relatively transparent to photons with present energy E_{γ_0} in the MeV range, the dominant absorption process being pair production on neutral matter. Compton scattering energy losses become important for $E_{\gamma_0} \lesssim 0.1$ MeV, while $\gamma-\gamma$ scattering rapidly increases the opacity for $E_{\gamma_0} \gtrsim 100$ MeV and pair production for $E_{\gamma_0} \gtrsim 1$ GeV [31]. The total optical depth is relatively constant with energy in the observed range $\sim 0.3 - 200$ MeV, reaching unity at a redshift

$$z \lesssim z_{abs} \simeq 420\Omega^{\frac{1}{3}}\left[\left(\frac{\Omega_N}{0.1}\right)h\right]^{-\frac{2}{3}}. \qquad (54)$$

Hence absorption can be sensibly neglected for γ-rays with *present* energy in the MeV range emitted by decaying particles with lifetimes

$$\frac{\tau_x}{t_0} \gtrsim 10^{-4}. \qquad (55)$$

The observed intensity of the diffuse extragalactic γ-ray background [41] can be represented approximately by the power law

$$\frac{dJ}{dE_{\gamma_0}} \simeq 10^{-2}\ (\mathrm{cm^2\ sec\ st\ MeV})^{-1}\left(\frac{E_{\gamma_0}}{\mathrm{MeV}}\right)^{-2.3}, \qquad (56)$$

for $E_{\gamma_0} \sim 0.1-1$ MeV and $\sim 10-200$ MeV. At intermediate energies, there is a 'bump' described approximately by the power law $\sim E_{\gamma_0}^{-1}$, for $E_{\gamma_0} \sim 1-3$ MeV, steepening to $\sim E_{\gamma_0}^{-2.5-3}$ between 3 and 10 MeV. In calculating the constraints below, we have used the actual (90% c.l.) upper bounds to the γ-ray flux obtained by the *Apollo-11* experiment in the 0.3–10 MeV range [42], and by the *SAS-II* experiment in the 35–170 MeV range (after subtraction of the high-latitude galactic component) [43].

Consider a relic population of massive particles decaying isotropically into γ-rays with branching ratio B_γ. If the particle is massive enough the universe would be optically thick to the primary decay photons which would then trigger radiation cascades in the manner described in Section 3; only the 'breakout' photons below the threshold for pair production would be able to propagate to the present epoch. Assuming that the decays all occur at $t = \tau_x$ and that the average energy of the decay photons is $\langle E_\gamma\rangle = m_x/3$, cascades will be generated if

$$m_x \gtrsim m_{crit} \sim 1.5\times 10^5\ \mathrm{GeV}\ \left(\frac{\tau_x}{t_0}\right)^{\frac{2}{3}}, \qquad (57)$$

where we have used eq. (7) for the threshold energy E_{max}. However, the cascade spectrum will no longer be given as before by eq. (11) if the decay redshift is less than ~ 300 (corresponding to $\tau_x/t_0 \gtrsim 2\times 10^{-4}$), since $\gamma-\gamma$ scattering now becomes unimportant. The spectrum now falls as $\sim E_\gamma^{-1.5}$ until $\sim 0.04E_{max}$ and then steepens to $\sim E_\gamma^{-1.8}$ before being cut off at E_{max} [30]. This complicates the analysis, but in practice little error is made if we continue to use eq. (11) since th observed spectrum is steeper than either cascade spectrum (for $E_\gamma \ll E_{max}$). With the assumption made above for the average energy of the decay photons, the source spectrum *per* decaying particle is

$$\mathcal{S}(E_\gamma) \simeq \begin{cases} \frac{8\sqrt{2}}{55}B_\gamma m_x E_{max}^{-\frac{1}{2}}E_\gamma^{-\frac{3}{2}} & \text{for } 0 \le E_\gamma \le E_{max}/2, \\ \frac{1}{55}B_\gamma m_x E_{max}^3 E_\gamma^{-5} & \text{for } E_{max}/2 \le E_\gamma \le E_{max}, \\ 0 & \text{for } E_\gamma > E_{max}, \end{cases} \qquad (58)$$

with the normalization $\int dE_\gamma E_\gamma \mathcal{S}(E_\gamma) = B_\gamma m_x/3$, where $B_\gamma(=f_\gamma m_x/\langle E_\gamma\rangle)$ is the branching ratio for radiative decays. On the other hand, when $m_x \ll m_{crit}$, the decay photons can propagate, without cascading, [10] down to the present epoch, and the source spectrum can be approximately taken to be a delta function

$$\mathcal{S}(E_\gamma) \simeq B_\gamma\ \delta(E_\gamma - \langle E_\gamma\rangle). \qquad (59)$$

[10] It is suggested in ref. [46] that, for particles decaying today, Compton scattering of decay *electrons* off the blackbody photons can generate a cascade-like photon spectrum even if the decay photons themselves are not above the pair production threshold. This is incorrect since the Compton scattering timescale is today $\sim 10^6$ times longer than the expansion age [see the remark following eq. (52)].

with $\langle E_\gamma \rangle = m_x/3$. The expected γ-ray flux from relic particle decays is

$$\frac{dJ}{dE_{\gamma_0}} \simeq \frac{1}{4\pi} \int_0^{z_{abs}} \frac{dz}{H_0(1+z)\sqrt{1+\Omega z}} S(E_\gamma) \frac{dn_x}{dt}, \tag{60}$$

where we have used $dt/dz = H_0^{-1}(1+z)^{-2}(1+\Omega z)^{-1/2}$ and $E_\gamma = E_{\gamma_0}(1+z)$. We further assume $\Omega = 1$ implying $H_0 = 2/3t_0$.

First, consider the case that the decaying particle is not massive enough to trigger radiation cascades. Taking the source spectrum to be given by eq. (59), the redshift-integrated present flux is

$$\frac{dJ}{dE_{\gamma_0}} \simeq \frac{3}{8\pi} B_\gamma \frac{n_x}{n_\gamma} n_\gamma(t_0) \frac{t_0}{\tau_x} \frac{E_{\gamma_0}^{\frac{1}{2}}}{\langle E_\gamma \rangle^{\frac{3}{2}}} \exp\left[-\left(\frac{t_0}{\tau_x}\right)\left(\frac{E_{\gamma_0}}{\langle E_\gamma \rangle}\right)^{\frac{3}{2}} \right], \tag{61}$$

subject to the bound (55) on the decay epoch. The spectral shape above is quite similar to the shape of the 'bump' in the observed spectrum at MeV energies [44,45]. The most generous constraint then follows from requiring that the expected flux not exceed the 90% c.l. observational upper limits in this region [42]. This yields the bound

$$B_\gamma \left(\frac{n_x}{n_\gamma}\right) \lesssim 1.4 \times 10^{-14},$$
$$\text{for } m_x \sim 7.5 \times 10^{-3} \left(\frac{\tau_x}{t_0}\right)^{-\frac{2}{3}}, \tag{62}$$

i.e. for $m_x \sim (0.01 - 3)$ GeV. This bound is shown as a dotted line in fig. 5, taking $B_\gamma = 1$. For more massive particles, upto the critical mass required to generate cascades [eq. (57)], the above bound becomes *more* stringent since the maximum in the spectrum (61) at $E_{\gamma_0} \simeq (m_x/3)(\tau_x/t_0)^{2/3}$ is now higher in energy than the observed 'bump' and is therefore bounded by the more restrictive power law extension [eq. (56)] at higher energies.

When the decaying particle is massive enough to generate cascades, the source spectrum is given by eq. (58). We need consider only the part of the spectrum below $E_{max}/2$ since the observed γ-ray spectrum has the slope ~ -2.3. Integrating eq. (60), we obtain for the expected spectrum today:

$$\frac{dJ}{dE_{\gamma_0}} \simeq \frac{1}{4\pi} 0.2 B_\gamma m_x \frac{n_x}{n_\gamma} n_\gamma(t_0) E_{max}^{-\frac{1}{2}}(t_0) E_{\gamma_0}^{-\frac{3}{2}} \left[1 - e^{-\left(\frac{t_0}{\tau_x}\right)\left(\frac{2E_{\gamma_0}}{E_{max}(t_0)}\right)^{\frac{3}{2}}} \right]. \tag{63}$$

The best bound comes from the highest observed energy of 170 MeV, where the 90% c.l. upper limit to the observed flux (after subtraction of the Galactic background) is 7×10^{-8} (cm^2 sec st MeV)$^{-1}$ [43]. Comparing this to the expected flux gives

$$B_\gamma \left(\frac{m_x}{\text{GeV}}\right)\left(\frac{n_x}{n_\gamma}\right) \lesssim 8.5 \times 10^{-15}. \tag{64}$$

We show this as a dashed line in fig. 5, taking $B_\gamma = 1$. This bound is a factor of ~ 3 more restrictive than the one obtained by Dodelson [46]. We have considered the cosmological propagation of γ-rays and the observational data in more detail.

6 Bounds from High Energy Neutrinos

The previous arguments constrain the relic abundance of massive unstable particles with lifetimes ranging from a tenth of a second up to a fraction of the age of the Universe ($t_0 \sim 2 \times 10^{17}$sec $h^{-1}(\frac{1}{3}\sqrt{\Omega} + \frac{2}{3})^{-1}$). Particles with lifetimes comparable to or longer than the present age would contribute to the dark matter; their energy density in ratio to the critical density is

$$\Omega_x h^2 \simeq 4 \times 10^7 \left(\frac{m_x}{\text{GeV}}\right)\left(\frac{n_x}{n_\gamma}\right). \tag{65}$$

The decays of such long lived particles would generate high energy neutrinos which can be observed by nucleon decay experiments (*IMB, Kamiokande, Fréjus, ...*) or cosmic ray observatories (*Fly's Eye, DUMAND, ...*). The non-observation of such a signal above the background expected from cosmic ray interactions in the atmosphere constrains the relic abundance of such particles and thereby determines their suitability as candidates for dark matter. This idea was originally suggested [47,48] before any experimental data were available. We present below the analytic formulation of such bounds as well as results obtained from numerical calculations [49] which are necessary to take various threshold and absorption effects into account [50].

We consider a population of relic massive particles decaying (isotropically) into neutrinos with a branching ratio B_ν. The present number density of the decay neutrinos with (present) energy E_{ν_0} above a given threshold E_{thr} is given by [11]

$$n_\nu(E_{\nu_0} > E_{thr}) = B_\nu n_x \int_{t_{min}}^{t_0} \frac{dt}{\tau_x} \exp\left(-\frac{t}{\tau_x}\right), \tag{66}$$

where $t_{min} = t_0(E_{thr}/E_\nu)^{3/2}$ restricts the integration to neutrinos which were emitted with energy E_ν at time t, and whose redshifted energy is above E_{thr} today. (The exponent 3/2 is for a matter-dominated Universe.) Changing variables from t to E_{ν_0}

$$n_\nu(E_{\nu_0} > E_{thr}) = B_\nu n_x \frac{3t_0}{2\tau_x} \int_{E_{thr}}^{E_\nu} \frac{dE_{\nu_0}}{E_\nu} \left(\frac{E_{\nu_0}}{E_\nu}\right)^{\frac{1}{2}} \exp\left[-\frac{t_0}{\tau_x}\left(\frac{E_{\nu_0}}{E_\nu}\right)^{\frac{3}{2}} \right]. \tag{67}$$

We have assumed that the Universe has been transparent to the emitted neutrinos for the neutrino energies and particle lifetimes to be considered. (The necessary corrections for scattering of very high energy neutrinos on the relic thermal neutrino background have been evaluated numerically [49].) Integrating eq. (67), the present day neutrino flux is

$$J_\nu(E_{\nu_0} > E_{thr}) = \frac{cn_\nu}{4\pi}$$
$$\simeq 3.1 \times 10^{19} \text{ (cm}^2 \text{ sr yr)}^{-1} B_\nu \left(\frac{n_x}{n_\gamma}\right) \left[\exp\left(-\frac{t_0}{\tau_x}\left(\frac{E_{thr}}{E_\nu}\right)^{\frac{3}{2}} \right) - \exp\left(-\frac{t_0}{\tau_x}\right) \right]. \tag{68}$$

[11] The particles are assumed to be uniformly distributed whereas they are likely to have clustered along with other matter into galaxies *etc.* A correction would only be necessary for particles decaying today ($\tau > t_0$) and, in case, would *improve* the bounds further.

Two kinds of events can be generated by high energy neutrinos in nucleon decay detectors — ***contained events*** which correspond to electron or muon neutrinos (or antineutrinos) producing the corresponding charged leptons through interactions with nucleons inside the detector, and ***throughgoing muons*** generated by muon neutrinos which interact with nucleons in the surrounding rock. In addition, cosmic ray observatories can directly detect the ***air showers*** triggered by the interaction of very high energy neutrinos in the Earth's atmosphere. Underwater detectors, presently under construction, will be able to detect neutrino generated cascades (*water showers ?!*) in deep lakes or in the sea.

The rate at which contained events are generated per kiloton of detector material is simply

$$R_\nu = 4\pi J_\nu N_{kt} \sigma_{\nu N} \,, \tag{69}$$

where $N_{kt} \simeq 10^9 N_A$ is the number of nucleons in a kiloton and $\sigma_{\nu N}$ is the inelastic scattering cross-section.

To obtain the rate of throughgoing muons, we need to know the 'penetration depth' X_μ, *viz.* the distance from which muons produced with energy E_μ may reach the detector. Taking into account the increased energy loss at energies in excess of $\mathcal{O}$(TeV) due to bremsstrahlung and photonuclear interactions, in addition to ionisation, this is [51]

$$X_\mu \simeq 0.5 \text{ km } \ln\left[1 + \frac{E_\mu}{0.5 \text{ TeV}}\right]. \tag{70}$$

(For $E_\mu \ll 1$ TeV, where ionisation loss is dominant, this becomes the more familiar expression $X_\mu \simeq 100\,\text{cm}\,(E_\mu/\text{GeV})$. For $E_\mu \gg 1$ TeV, the energy loss process becomes stochastic but eq. (70) still suffices for our purposes.) The flux of throughgoing muons per unit area of detector (of total area A) is then

$$J_\mu = 4\pi J_\nu \sigma_{\nu N} N_{kt} \rho_{rock} \frac{1}{A} \int_0^{X_\mu} 4\pi r^2 dr \left(\frac{A}{4\pi r^2}\right) = R_\nu X_\mu \rho_{rock} \,, \tag{71}$$

where $\rho_{rock} \simeq 5$ gm/cm^3. This expression does not take into account the absorption of high energy neutrinos in the Earth [52,53] which, however, has been incorporated in the numerical calculations [49].

The air shower observations set limits on the cross-section-integrated flux

$$\mathcal{J}(E_{th}) = \int_{E_{th}} \sigma_{\nu N}(E_{\nu_0}) \left(\frac{dJ_\nu}{dE_{\nu_0}}\right) dE_{\nu_0} \,, \tag{72}$$

where the differential flux is $dJ_\nu/dE_{\nu_0} = (c/4\pi)(dn_\nu/dE_{\nu_0})$.

The results obtained in refs. [51,54] allow convenient parametrizations of $\sigma_{\nu N}$ in the energy ranges: **(I)** $E_{\nu_0} < 3$ TeV, **(II)** 3 TeV $< E_{\nu_0} < 10^4$ TeV, and **(III)** $E_{\nu_0} > 10^4$ TeV. We shall evaluate bounds on the decaying particle abundance separately for these three ranges, using the best applicable observational limit in each case. We also consider separately the two cases: **(a)** $\tau_x < t_0$ where we approximate $1 - e^{-t_0/\tau_x} \simeq 1$, and $E_{\nu_0} \simeq E_\nu (\tau_x/t_0)^{\frac{2}{3}}$ (corresponding to the peak in the red-shifted decay spectrum), and **(b)** $\tau_x > t_0$ for which we take $1 - e^{-t_0/\tau_x} \simeq t_0/\tau_x$, and $E_{\nu_0} = E_\nu$. For both cases

we assume $E_\nu = m_x/3$. The numerical results [49] which are displayed in fig. 6 have been obtained without these approximations and also taking energy threshold effects into account. We give the analytically derived bounds below for comparison.

In energy ranges **I** and **II**, the best bounds come from the experimental upper limit on upward-going muons from the *IMB* detector [55,56]

$$\frac{J_\mu}{2} < 2.65 \times 10^{-13} \text{ (cm}^2 \text{ sec)}^{-1} \text{ at 90\% c.l., for } E_{thr} > 2 \text{ GeV}, \tag{73}$$

while less stringent bounds are obtained from the *IMB* limit on contained events [55,56]

$$R_\nu < 10^6 \text{ (Kton yr)}^{-1} \text{ at 90\% c.l., for } E_{thr} > \mathcal{O}(100) \text{ MeV}. \tag{74}$$

In the energy range **III**, the best bounds comes from the *Fly's Eye* observatory as soon as its detection threshold of 10^5 TeV is reached. For downward going neutrinos the bounds are [57,53]

$$\mathcal{J}(10^5 \text{ TeV}) < 10^{-45} \text{ (sec sr)}^{-1} \,; \qquad \mathcal{J}(10^7 \text{ TeV}) < 10^{-46} \text{ (sec sr)}^{-1} \,. \tag{75}$$

Let us first consider energy range **I** for which the charged current neutrino cross-section is [58]

$$\sigma_{\nu N} = \epsilon \times 10^{-38} \text{ cm}^2 \left(\frac{E_{\nu_0}}{\text{GeV}}\right), \tag{76}$$

where $\epsilon \simeq 0.67$ (0.34) for neutrinos (antineutrinos). From eq. (69), the rate of contained events is then given by

$$R_\nu \simeq 1.2 \times 10^{15} \text{ (kton yr)}^{-1} B_\nu \left(\frac{n_x}{n_\gamma}\right) \epsilon \left(\frac{E_{\nu_0}}{\text{GeV}}\right) (1 - e^{-t_0/\tau_x}). \tag{77}$$

Taking $B_\nu = B_{\nu_e} + B_{\bar{\nu}_e} + B_{\nu_\mu} + B_{\bar{\nu}_\mu} = 4\bar{B}_\nu$, the experimental limit (74) on R_ν implies: for **(a)** $\tau_x < t_0$,

$$\bar{B}_\nu \left(\frac{m_x}{\text{GeV}}\right) \left(\frac{n_x}{n_\gamma}\right) < 10^{-13} \left(\frac{t_0}{\tau_x}\right)^{\frac{2}{3}}, \tag{78}$$

and, for **(b)** $\tau_x > t_0$,

$$\bar{B}_\nu \left(\frac{m_x}{\text{GeV}}\right) \left(\frac{n_x}{n_\gamma}\right) < 10^{-13} \left(\frac{\tau_x}{t_0}\right). \tag{79}$$

The last can also be written as

$$\Omega_x h^2 < 4 \times 10^{-6} \bar{B}_\nu^{-1} \left(\frac{\tau_x}{t_0}\right), \tag{80}$$

valid for $m_x \lesssim 10$ TeV.

Similarly, the rate of throughgoing muons is

$$J_\mu \simeq 10^4 \text{ (cm}^2 \text{ sec)}^{-1} \; B_\nu \left(\frac{n_x}{n_\gamma}\right) \epsilon \left(\frac{E_{\nu_0}}{\text{GeV}}\right) \ln\left[1 + \frac{E_\mu}{0.5 \text{ TeV}}\right] (1 - e^{-t_0/\tau_x}). \tag{81}$$

Taking $B_\nu = B_{\nu_\mu} + B_{\bar{\nu}_\mu} = 2\bar{B}_\nu$, the experimental limit (73) on J_μ now gives: for **(a)** $\tau_x < t_0$,

$$\bar{B}_\nu \left(\frac{m_x}{\text{GeV}}\right)\left(\frac{n_x}{n_\gamma}\right) < 10^{-17} F_{abs} \left(\frac{t_0}{\tau_x}\right)^{\frac{2}{3}} \ln^{-1}\left[1 + \frac{m_x}{1.5\text{ TeV}}\left(\frac{\tau_x}{t_0}\right)^{\frac{2}{3}}\right], \tag{82}$$

and, for **(b)** $\tau_x > t_0$,

$$\bar{B}_\nu \left(\frac{m_x}{\text{GeV}}\right)\left(\frac{n_x}{n_\gamma}\right) < 10^{-17} F_{abs} \left(\frac{\tau_x}{t_0}\right) \ln^{-1}\left[1 + \frac{m_x}{1.5\text{ TeV}}\right], \tag{83}$$

or, equivalently,

$$\Omega_x h^2 < 4 \times 10^{-10} F_{abs} \bar{B}_\nu{}^{-1} \left(\frac{\tau_x}{t_0}\right) \ln^{-1}\left[1 + \frac{m_x}{1.5\text{ TeV}}\right], \tag{84}$$

valid for $m_x \lesssim 10$ TeV. Here, F_{abs} is a correction for absorption in the Earth, which is numerically calculated [49] to be of $\mathcal{O}(10)$. We show these bounds in fig. 6 for $m_x = 1$ TeV (taking $\bar{B}_\nu = 1$). Threshold effects cause the turnover at small lifetimes.

For energy range **II**, the neutrino cross-section is well approximated (within $\sim$ 50% of the values given in ref. [59]) by

$$\sigma_{\nu N} \simeq 2 \times 10^{-35}\text{ cm}^2 \left(\frac{E_{\nu_0}}{3\text{ TeV}}\right)^{\frac{1}{2}}. \tag{85}$$

The antineutrino cross-section is $\sim 1/2$ of the above at the lower end of the range, but equals the neutrino cross-section for energies in excess of 100 TeV. Thus the contained event rate is now

$$R_\nu \simeq 3.6 \times 10^{18}(\text{kton yr})^{-1} B_\nu \left(\frac{n_x}{n_\gamma}\right)\left(\frac{E_{\nu_0}}{3\text{ TeV}}\right)^{\frac{1}{2}} (1 - e^{-t_0/\tau_x}). \tag{86}$$

With $B_\nu = 4\bar{B}_\nu$ as before, the bounds which follow from the limit (74) on R_ν are: for **(a)** $\tau_x < t_0$,

$$\bar{B}_\nu \left(\frac{m_x}{\text{GeV}}\right)\left(\frac{n_x}{n_\gamma}\right) < 10^{-13} \left(\frac{t_0}{\tau_x}\right)^{\frac{1}{3}} \left(\frac{m_x}{10\text{ TeV}}\right)^{\frac{1}{2}}, \tag{87}$$

and, for **(b)** $\tau_x > t_0$

$$\bar{B}_\nu \left(\frac{m_x}{\text{GeV}}\right)\left(\frac{n_x}{n_\gamma}\right) < 10^{-13} \left(\frac{\tau_x}{t_0}\right) \left(\frac{m_x}{10\text{ TeV}}\right)^{\frac{1}{2}}, \tag{88}$$

which can also be written as

$$\Omega_x h^2 < 4 \times 10^{-6} \bar{B}_\nu{}^{-1} \left(\frac{\tau_x}{t_0}\right) \left(\frac{m_x}{10\text{ TeV}}\right)^{\frac{1}{2}}, \tag{89}$$

valid for 10 TeV $\lesssim m_x \lesssim 3 \times 10^4$ TeV.

The rate of throughgoing muons is now

$$J_\mu \simeq 3 \times 10^7\text{ (cm}^2\text{ sec)}^{-1}\ B_\nu \left(\frac{n_x}{n_\gamma}\right)\left(\frac{E_{\nu_0}}{3\text{ TeV}}\right)^{\frac{1}{2}} \ln\left[1 + \frac{E_\mu}{0.5\text{ TeV}}\right](1 - e^{-t_0/\tau_x}). \tag{90}$$

Taking $B_\nu = 2\bar{B}_\nu$ as is appropriate for this case, the limit (73) on J_μ yields: for **(a)** $\tau_x < t_0$,

$$\bar{B}_\nu \left(\frac{m_x}{\text{GeV}}\right)\left(\frac{n_x}{n_\gamma}\right) < 10^{-17} F_{abs} \left(\frac{t_0}{\tau_x}\right)^{\frac{1}{3}} \left(\frac{m_x}{10\text{ TeV}}\right)^{\frac{1}{2}} \ln^{-1}\left[1 + \frac{m_x}{1.5\text{ TeV}}\left(\frac{\tau_x}{t_0}\right)^{\frac{2}{3}}\right], \tag{91}$$

and, for **(b)** $\tau_x > t_0$,

$$\bar{B}_\nu \left(\frac{m_x}{\text{GeV}}\right)\left(\frac{n_x}{n_\gamma}\right) < 10^{-17} F_{abs} \left(\frac{\tau_x}{t_0}\right) \left(\frac{m_x}{10\text{ TeV}}\right)^{\frac{1}{2}} \ln^{-1}\left[1 + \frac{m_x}{1.5\text{ TeV}}\right]. \tag{92}$$

or, equivalently

$$\Omega_x h^2 < 4 \times 10^{-10} F_{abs} \bar{B}_\nu{}^{-1} \left(\frac{\tau_x}{t_0}\right) \left(\frac{m_x}{10\text{ TeV}}\right)^{\frac{1}{2}} \ln^{-1}\left[1 + \frac{m_x}{1.5\text{ TeV}}\right], \tag{93}$$

valid for 10 TeV $\lesssim m_x \lesssim 3 \times 10^4$ TeV. The corresponding numerically obtained bounds [49] are shown in fig. 6 for $m_x = 10^3$ TeV (assuming $\bar{B}_\nu = 1$).

In energy range **III**, the cross-section changes slowly enough [60,59,54] that it is reasonably approximated by

$$\sigma_{\nu N}(E_\nu) \simeq \sigma_{\nu N}(E_{th}) \left(\frac{E_\nu}{E_{th}}\right)^a, \tag{94}$$

where $a \simeq 0.35$ and $\sigma(E_{th}) \simeq 3.4 \times 10^{-33}$ cm^2 for $E_{th} = 10^5$ TeV, and $a \simeq 0.24$ and $\sigma(E_{th}) \simeq 1.5 \times 10^{-32}$ cm^2 for $E_{th} = 10^7$ TeV [59]. When $\tau_x < t_0$, dJ_ν/dE_{ν_0} is a steeply falling function of E_{ν_0} so that we may replace $\sigma_{\nu N}(E_{\nu_0})$ by $\sigma_{\nu N}(E_{th})$, obtaining

$$\mathcal{J}(E_{th}) \simeq \sigma_{\nu N}(E_{th}) J_\nu(E_{th}). \tag{95}$$

However the bound thus obtained is not very good because for such high energy neutrinos the opacity of the early universe cannot be neglected. The absorption due to scattering on the relic thermal neutrino background must be calculated numerically [49]. Such corrections are not required when $\tau_x > t_0$ for which we have

$$\mathcal{J}(E_{th}) \simeq \frac{B_\nu}{4\pi} n_x \frac{3t_0}{2\tau_x} E_\nu^{\frac{3}{2}} \int_{E_{th}}^{E_\nu} \sigma_{\nu N}(E_{\nu_0}) E_{\nu_0}^{\frac{1}{2}} dE_{\nu_0}. \tag{96}$$

Using the experimental limit (75), this requires for $E_{th} = 10^5$ TeV,

$$\bar{B}_\nu \left(\frac{m_x}{\text{GeV}}\right)\left(\frac{n_x}{n_\gamma}\right) < 3 \times 10^{-17} \left(\frac{\tau_x}{t_0}\right) \left(\frac{m_x}{3 \times 10^5\text{ TeV}}\right)^{\frac{2}{3}}, \tag{97}$$

valid for $m_x \gg 10^5$ TeV, and for $E_{th} = 10^7$ TeV,

$$\bar{B}_\nu \left(\frac{m_x}{\text{GeV}}\right)\left(\frac{n_x}{n_\gamma}\right) < 7 \times 10^{-18} \left(\frac{\tau_x}{t_0}\right) \left(\frac{m_x}{3 \times 10^7\text{ TeV}}\right)^{\frac{3}{4}}. \tag{98}$$

valid for $m_x \gg 10^7$ TeV. The last can also be expressed as

$$\Omega_x h^2 < 3 \times 10^{-10} \bar{B}_\nu^{-1} \left(\frac{\tau_x}{t_0}\right) \left(\frac{m_x}{3 \times 10^7 \text{ TeV}}\right)^{\frac{3}{4}}. \quad (99)$$

This bound is within a factor of ~ 2 of that calculated numerically [49] which is shown in fig. 6 for $m_x = 10^{10}$ GeV. It is clear that a metastable relic particle of such a mass may indeed constitute the dark matter if its lifetime exceeds $\sim 10^{16}$ yr.

7 Constraints on Proposed Particles

The bounds derived and compiled above can in principle be applied to any conjectured species of massive unstable particle. To illustrate how they can be used to constrain particle properties, we choose to discuss two specific cases: technicolour 'baryons' [7] and 'cryptons' (bound states in the hidden sector of a superstring-derived model) [8].

A generic technicolour scenario invokes new hyperstrong interactions with an intrinsic scale of $\Lambda_{TC} \sim 0.5 - 1$ TeV, due to gauge interactions with $N_{TC} \geq 3$ unbroken technicolours. These gauge interactions bind tecchniquarks Q_T in the fundamental N_{TC} representation of $SU(N_{TC})$, forming $Q_T \bar{Q}_T$ 'technimeson' and $Q_T^{N_{TC}}$ 'technibaryon' bound states. The latter will have integer spin if N_{TC} is even, and the choice often favoured is $N_{TC} = 4$. The lightest technimeson would be expected to be short-lived with $\tau \ll 1$ sec, thus evading our cosmological bounds, but the lightest technibaryon, which has a mass

$$m_{TB} \simeq m_p \left(\frac{\Lambda_{TC}}{\Lambda_{QCD}}\right) \simeq m_p \left(\frac{v}{f_\pi}\right) \simeq 2.5 \text{ TeV}, \quad (100)$$

is likely to be metastable, by analogy with the proton of QCD.

Indeed, as in QCD, there is no renormalizable interaction that can cause technibaryon decay. However, the minimal technicolour model must in any case be extended to incorporate quark and lepton masses [7], and one could anticipate that it should be unified in some kind of techni-GUT. Therefore one expects, in general, higher-order effective non-renormalizable interactions that cause technibaryon decay, of the form

$$\mathcal{L}_{TBX} = \frac{Q_T^{N_{TC}} f^n}{M^{3/2(N_{TC}+n)-4}} \quad (101)$$

where f is a quark or lepton field and M some mass scale $\gg \Lambda_{TC}$ at which the effective interaction is generated. These would imply a technibaryon lifetime

$$\tau_{TB} \simeq \frac{1}{\Lambda} \left(\frac{M}{\Lambda}\right)^{3(N_{TC}+n)-8}. \quad (102)$$

For the favoured case $N_{TC} = 4$ with the minimum choice $n = 0$ one finds

$$\tau_{TB} \sim 10^{-27} \text{ sec } \left(\frac{M}{\Lambda}\right)^4, \quad (103)$$

which is $\sim 3 \times 10^{17}$ yr for $M \sim 10^{16}$ GeV.

Estimating the self-annihilation cross-section of technibaryons to be given by

$$\langle \sigma v \rangle_{TB} \simeq \langle \sigma v \rangle_{p\bar{p}} (m_p/m_{TB})^2 \simeq 3 \times 10^{-5} \text{ GeV}^2, \quad (104)$$

the *minimum* expected relic abundance is $m_{TB} n_{TB}/n_\gamma \simeq 3 \times 10^{-13}$ GeV, having accounted for entropy generation following 'freeze-out' at ~ 70 GeV. As can be seen in the figures, unstable technibaryons with such an abundance may have any lifetime up to $\sim 10^{13}$ sec without affecting primordial nucleosynthesis or the 2.7 ^{0}K radiation, in agreement with the earlier analysis by Dodelson [46]. However, longer lifetimes up to $\sim 10^{13}$ yr are excluded by the constraints from the diffuse gamma ray background [46] as well as by the bounds on high energy neutrinos. These correspond to the constraints

$$M \lesssim 10^{13} \text{ GeV} \qquad \text{or} \qquad M \gtrsim 10^{15} \text{ GeV}. \quad (105)$$

The former case might be applicable to any extended technicolour model containing interactions that violate technibaryon number, while the latter case could accomodate a techni-GUT. Indeed, it is amusing that the lower boundon M in this case is close to the usual grand unification scale.

Technibaryons may have a higher relic density, which is cosmologically significant, if there is a technibaryon – anti-technibaryon asymmetry of the same order as the baryon – anti-baryon asymmetry [61]. Recently a natural mechanism for generating such an asymmetry has emerged with the realisation that non-perturbative processes in the Standard Model cause unsuppressed fermion number violation at temperatures above the electroweak scale. This would distribute any pre-existing fermion number among *all* electroweak doublets. If such processes cease being important below a temperature $T_* \simeq 300$ GeV, then the technibaryon to baryon ratio, which is suppressed by a factor $[m_{TB}(T_*)/T_*]^{3/2} \exp -[m_{TB}(T_*)/T_*]$, is just right to give $\Omega_{TB} \simeq 1$ [62]. Although technibaryons with masses upto a few TeV are experimentally ruled out as constituents of the Galactic dark matter if they have *coherent* weak interactions [63], the lightest technibaryon may well be an electroweak singlet (in addition to being charge and colour neutral) and hence unconstrained by direct searches. However relic technibaryons with the critical density are excluded by our astrophysical bounds, as seen in fig. 6, unless $\tau_{TB} \gtrsim 10^{18}$ yr, corresponding to $M \gtrsim 10^{16}$ GeV.

The same considerations apply to other heavy metastable particles which have been proposed as dark matter candidates, motivated by a preliminary report of an anomalous component of positrons (of energy > 10 GeV) in cosmic rays. These positrons may have resulted from the decay of ~ 30 GeV right-handed neutrinos [64] or $1 - 3$ TeV mass particles [65], with a lifetime of $\sim 10^{17}$ yr.

We conclude by discussing the decays of 'cryptons' in the flipped $SU(5)$ model [66], which contains two confining non-Abelian gauge factors: $SO(10)$ which becomes strong at $\Lambda_{10} \sim 10^{15}$ GeV, and $SU(4)$ which becomes strong at $\Lambda_4 \sim 10^{12}$ GeV. There are hidden $SO(10)$ mesons which are bound states $T_i T_j (i,j = 1 \text{ to } 5)$ of $\underline{10}$ representations, and $SU(4)$ mesons: $\Delta_i \Delta_j (i,j = 1 \text{ to } 5)$ and $\tilde{F}_i \tilde{F}_j (i,j = 1 \text{ to } 6)$ made of $\underline{6}\,\Delta_i$ and $\underline{4}(\bar{\underline{4}})\,\tilde{F}_i(\tilde{\bar{F}}_i)$ constituents, baryons $\tilde{F}_i \tilde{F}_j \Delta_k$ and $\tilde{\bar{F}}_i \tilde{\bar{F}}_j \Delta_k$, and four-constituent 'tetrons' $\tilde{F}_i \tilde{F}_j \tilde{F}_k \tilde{F}_l$ and $\tilde{\bar{F}}_i \tilde{\bar{F}}_j \tilde{\bar{F}}_k \tilde{\bar{F}}_l$. We expect some of the constituents:

$\Delta_3, T_3, \bar{F}_3, \bar{\bar{F}}_3, \bar{F}_5, \bar{\bar{F}}_5$ to have masses much less than $\Lambda_4 \sim 10^{12}$ GeV, causing the corresponding mesons to be light à la the pion of QCD, but the other states should weigh $\gtrsim \Lambda_{10}$ (for the other $T_i T_j$ mesons), or $\gtrsim \Lambda_4$ (for the remaining $SU(4)$ bound states).

The constituent fields have very few renormalizable third-order ($N = 3$) superpotential interactions, so most of these states can only decay via higher-order ($N \geq 4$) superpotential terms. Generically, we expect crypton lifetimes to be

$$\tau_x \simeq \frac{1}{m_x}\left(\frac{M}{m_x}\right)^{2(N-3)}, \quad m_x \sim \Lambda, \tag{106}$$

with, according to recent calculations [67], $M \sim 10^{18}$ GeV, leading to

$$\tau_{10} \sim 10^{(6N_{10}-65)} \text{ yr}, \quad \tau_4 \sim 10^{(12N_4-80)} \text{ yr}, \tag{107}$$

for $SO(10)$ and $SU(4)$ bound states respectively. Thus $\tau_{10} \gtrsim 1$ sec (10^{16} yr) for $N_{10} \geq 10\,(14)$ and $\tau_4 \gtrsim 1$ sec (10^{16} yr) for $N_4 \geq 6\,(8)$.

We find many fourth- and fifth-order interactions leading to decays of $SO(10)$ mesons, [12] and expect the majority of these to be highly unstable since it requires stability against at least tenth-order interactions to have $\tau_{10} \gtrsim 1$ sec [see eq.(107)]. However, many of the $SU(4)$ mesons could be long-lived, with 7 $\Delta_i \Delta_j$ and 17 $\bar{F}_i \bar{\bar{F}}_j$ mesons having no $N \leq 5$ interactions, [12] and hence having lifetimes $\tau_4 \gtrsim 1$ sec. Similarly, only 23 $SU(4)$ baryons have $N_4 \leq 5$ decay interactions [12] so that $\tau_4 \lesssim 1$ sec, leaving 187 baryons with $\tau_4 \gtrsim 1$ sec. Even more strikingly, only the 2233 and $\bar{1}\bar{1}\bar{3}\bar{3}$ (3445) $SU(4)$ tetrons have $n_4 = 5\,(6)$ decay interactions, at most 50 have $N_4 = 7$, and at least 199 have $N_4 \geq 8$. All the latter are good candidates to have lifetimes $\tau_4 \gtrsim 10^{16}$ yr. In this case, as discussed in earlier sections, these metastable cryptons could, in principle, constitute the dark matter. [13]

A complete analysis of all the possible mass terms and decay channels for cryptons in the flipped $SU(5)$ model would confront enormous combinatorial problems, and it seems premature to undertake this task at the present time. Nevertheless, the model gives us the clear message that metastable cryptons with lifetimes $\gtrsim 10^{16}$ yr are quite plausible. Whether this particular model can avoid problems with metastable states having 1 sec $\lesssim \tau_x \lesssim 10^{16}$ yr is a question that requires more detailed investigation [68].

Acknowledgement We thank Savas Dimopoulos and Dave Seckel for clarification of their previous work on unstable relics. Three of us (G.B.G., D.V.N. and S.S.) thank the CERN Theoretical Physics Division for its hospitality while this work was started.

[12] Fourth-order $T_3 T_4$ interactions should be added to eq. (6) and fifth-order $\bar{F}_{1,5}\bar{\bar{F}}_6$ interactions to eq. (8) of ref. [8]. Additionally, the 121, 131, 231, $\bar{1}\bar{6}\bar{2}$ and $\bar{1}\bar{6}\bar{5}$ baryons should be added to the list given in that paper.

[13] We do not discuss in this paper the expected relic abundances of such metastable cryptons, which depends, in particular, on the entropy released in decays of less-stable cryptons [8].

References

[1] V. Trimble, Ann. Rev. Astron. Astrophys. 25(1987)425; J. Binney and S. Tremaine, *Galactic Dynamics*, Princeton University Press (1988).

[2] J. Rich, D. Lloyd-Owen, and M. Spiro, Phys. Rep. 151(1987)239; P.F. Smith, Contemp. Phys. 29(1988)159.

[3] J. Ellis, J.S. Hagelin, D.V. Nanopoulos, K.A. Olive and M. Srednicki, Nucl. Phys. B238(1984)453.

[4] A. De Rujula, S. Glashow and U. Sarid, Nucl. Phys. B333(1990)173; S. Dimopoulos, D. Eichler, R. Esmailzadeh and G. Starkman, Phys. Rev. D41(1990)2388; S.W. Barwick, P.B. Price and D.P. Snowden-Ifft, Phys. Rev. Lett. 64(1990)2859; R.S. Chivukula, A.G. Cohen, S. Dimopoulos and T.P. Walker, Phys. Rev. Lett. 65(1990)957.

[5] A. Gould, B.T. Draine, R.W. Romani and S. Nussinov, Phys. Lett. 238B(1990)337.

[6] K. Griest and J. Silk, Nature 343(1990)26; L.M. Krauss, Phys. Rev. Lett. 64(1990)999; J. Ellis, D.V. Nanopoulos, L. Roszkowski and D.N. Schramm, Phys. Lett. 245B(1990)251.

[7] E. Farhi and L. Susskind, Phys. Rep. 74(1981)277; R.K. Kaul, Rev. Mod. Phys. 55(1983)449.

[8] J. Ellis, J.L. Lopez and D.V. Nanopoulos, Phys. Lett. B247(1990)257.

[9] L.J. Hall, Proc. 16th SLAC Summer Institute on Particle Physics, ed. E.C. Brennan (1988) p. 85; K. Griest and M. Kamionkowski, Phys. Rev. Lett. 64(1990)615.

[10] D.N. Schramm and R.V. Wagoner, Ann. Rev. Nucl. Sci. 27(1977)37; J. Bernstein, L.S. Brown and G. Feinberg, Rev. Mod. Phys. 61(1988)25; K.A. Olive, D.N. Schramm, G. Steigman and T. Walker, Phys. Lett. B236(1990)454 and references therein.

[11] A.M. Boesgaard and G. Steigman, Ann. Rev. Astron. Astrophys. 23(1985)319.

[12] B.E.J. Pagel, in *A Unified View of the Macro- and Micro- Cosmos*, eds. A. De Rujula *et al*, World-Scientific Press (1988); in *Evolutionary Phenomena in Galaxies*, eds. J. Beckman *et al*, Cambridge University Press (1990).

[13] G.A. Shields, in *Proc. 13th Texas Symposium on Relativistic Astrophysics*, ed. P. Ulmer, World-Scientific Press (1988).

[14] S.M. Faber and J.S. Gallagher, Ann. Rev. Astron. Astrophys. 17(1979)135.

[15] G.A. Efstathiou, R.S. Ellis and B.A. Paterson, Mon. Not. R. astr. Soc. 232(1988)431.

[16] S. Sarkar and A.M. Cooper, Phys. Lett. 148B(1984)347.

[17] E.W. Kolb and R.J. Scherrer, Phys. Rev. D25(1982)1481.

[18] J. Ellis, D.V. Nanopoulos and S. Sarkar, Nucl. Phys. B259(1985)175.

[19] R.J. Scherrer and M.S. Turner, Astrophys. J. 331(1988)19.

[20] D. Lindley, Astrophys. J. 294(1985)1.

[21] M.Yu. Khlopov and A.D. Linde, Phys. Lett. 138B(1984)265.

[22] I. Halm, Phys. Lett. 188B(1987)403.

[23] R. Dominguez-Tenreiro, Astrophys. J. 313(1987)523.

[24] S. Dimopoulos, R. Esmailzadeh, L.J. Hall and G.D. Starkman, Astrophys. J. 330(1988)545.

[25] M.H. Reno and D. Seckel, Phys. Rev. D37(1988)3441.

[26] R. Juszkiewicz, J. Silk and A. Stebbins, Phys. Lett. 158B(1985)463.

[27] S. Dimopoulos, R. Esmailzadeh, L.J. Hall and G.D. Starkman, Nucl. Phys. B311(1989)699.

[28] M. Kawasaki and K. Sato, Phys. Lett. 189B(1987)23.

[29] F.A. Aharonian, V.G. Kirillov-Ugryumov and V.V. Vardanian, Astrophys. Sp. Sci. 115(1985)201.

[30] A. Zdziarski, Astrophys. J. 335(1988)786.

[31] A. Zdziarski and R. Svensson, Astrophys. J. 344(1989)551.

[32] R. Svensson and A. Zdziarski, Astrophys. J. 349(1990)415.

[33] L.M. Krauss and P. Romanelli, Astrophys. J. 358(1990)47.

[34] J.C. Mather *et al*, Astrophys. J. 354(1990)L37.

[35] H.P. Gush, M. Halpern and E.H. Wishnow, Phys. Rev. Lett. 65(1990)537.

[36] G.F. Smoot *et al*, Astrophys. J. 331(1988)537.

[37] P.J.E. Peebles, *Physical Cosmology*, Princeton University Press (1971); R.A. Sunyaev and Ya.B. Zeldovich, Ann. Rev. Astron. Astrophys. 18(1980)537; G. De Zotti, Prog. Nucl. Part. Phys. 17(1986)117; S. Sarkar, Rep. Prog. Phys. (1991) to appear.

[38] A.P. Lightman; Astrophys. J. 244(1981)392.

[39] P. Salati, E. Massó and S. Sarkar, in preparation.

[40] T. Matsumoto *et al*, Astrophys. J. 329(1988)567.

[41] J.I. Trombka and C.E. Fichtel, Phys. Rep. 97(1983)173.

[42] J.I. Trombka *et al*, Astrophys. J. 212(1977)925; see also V. Schönfelder, F. Graml and F.-P. Penningsfeld, Astrophys. J. 240(1980)350.

[43] C.E. Fichtel *et al*, Astrophys. J. 217(1977)L9; *ibid* 222(1978)833; D.J. Thompson and C.E. Fichtel, Astron. Astrophys. 109(1982)352.

[44] K.A. Olive and J. Silk, Phys. Rev. Lett. 55(1985)2362; *ibid*, 56(1986)2552.

[45] R. A. Daly, Astrophys. J. 324(1988)L47.

[46] S. Dodelson, Phys. Rev. D40(1989)3252.

[47] P.H. Frampton and S.L. Glashow, Phys. Rev. Lett. 44(1980)1481.

[48] J. Ellis, T.K. Gaisser and G. Steigman, Nucl. Phys. B177(1981)427.

[49] G.B. Gelmini, P. Gondolo and S. Sarkar, in preparation.

[50] V.S. Berezinskii, V.A. Dogiel, V.L. Ginzburg and V.S. Ptuskin, *Astrophysics of Cosmic Rays* (Elsevier 1990), Chapter VIII; V.S. Berezinsky, Bartol preprint BA-90-87 (1990).

[51] T.K. Gaisser and A.F. Grillo, Phys. Rev. D36(1987)2752.

[52] V.C. Berezinskii, A.Z. Gazizov, G.T. Zatsepin and I.L. Rozental, Sov. J. Nucl Phys. 43(1986)637.

[53] M.H. Reno and C. Quigg, Phys. Rev. D37(1988)657.

[54] A.V. Butkevich, A.B. Kaidalov, P.I. Krastev, A.V. Leonov-Vendrovski and I.M. Zheleznykh, Z. Phys. C39(1988)241.

[55] J.M. LoSecco *et al*, Phys. Lett. 188B(1987)388; R. Svoboda *et al*, Astrophys. J. 315(1987)420.

[56] R.M. Bionta *et al*, Phys. Rev. D38(1988)768.

[57] R.M. Baltrusaitis *et al*, Phys. Rev. D31(1985)2192.

[58] Particle Data Group, Phys. Lett. 239B(1990)1.

[59] C. Quigg, M.H. Reno and T.P. Walker, Phys. Rev. Lett. 57(1986)774.

[60] D.W. McKay and J.P. Ralston, Phys. Lett. 167B(1986)103.

[61] S. Nussinov, Phys. Lett. B165(1985)55; *ibid* B179(1986)103.

[62] S.M. Barr, R.S. Chivukula and E. Farhi, Phys. Lett. B241(1990)387.

[63] S.P. Ahlen *et al*, Phys. Lett. 195(1987)603; D.O. Caldwell *et al*, Phys. Rev Lett. 61(1988)510; F. Boehm *et al*, Phys. Lett. B255(1991)143.

[64] K.S. Babu, D. Eichler and R.N. Mohapatra, Phys. Lett. B226(1989)347.

[65] D. Eichler, Phys. Rev. Lett. 22(1989)2440.

[66] I. Antoniadis, J. Ellis, J. Hagelin and D.V. Nanopoulos, Phys. Lett. 231B(1989)65.

[67] S. Kalara, J. Lopez and D.V. Nanopoulos, Phys. Lett. 245B(1990)421, Nucl. Phys. B353(1991)650.

[68] J.Ellis, J. Lopez, D.V. Nanopoulos and K. Yuan, in preparation.

Figure Captions

Figure 1. Upper bounds on the decaying particle abundance as a function of its lifetime from the effects of entropy generation on primordial nucleosynthesis yields. Above the full line ^4He is overproduced, while above the dashed line ($D + {}^3He$) is overproduced [19]. The dotted line shows the approximate bound of eq. (5) [18]. These bounds apply for $m_x \gtrsim 1$ MeV.

Figure 2. Normalised rates for photodissociation of light elements (as labelled) by electromagnetic cascades generated by massive decaying particles, as functions of their lifetimes.

Figure 3. Upper bounds on the decaying particle abundance as a function of its lifetime from the effects of electromagnetic and hadronic cascades on primordial elemental abundances. For decays occuring after nucleosynthesis, the most severe constraints are from photoproduction of $D + {}^3He$ (eq. (18)) and photodestruction of D (eq. (19)). All these bounds apply for $m_x \gtrsim$ 10-50 MeV. The horizontal dashed line is the approximate bound given earlier [18] while the dotted line is the bound obtained in ref. [27]. For shorter lifetimes, the best bounds come from consideration of the production of ^4He and $D+{}^3He$ by hadronic cascades for $m_x \gtrsim 1$ GeV. [25].

Figure 4. Upper bounds on the decaying particle abundance as a function of its lifetime from the effects of radiative decays on the spectrum of the 2.7 ^{0}K background radiation. Above the full line an excessive chemical potential would be generated while above the dashed line there would be an observable distortion beyond the Wien peak (eq. (53)). The dotted line indicates the relaxation of the bound as the thermalization epoch is approached, according to the numerical calculations of ref. [26]. These bounds apply for $m_x \gtrsim 1$ MeV.

Figure 5. Upper bounds on the decaying particle abundance as a function of its lifetime from limits on the diffuse extragalactic γ-ray background radiation. The dotted line indicates the bound for particles of mass $\sim 0.01(\tau_x/t_0)^{-\frac{2}{3}}$ GeV whose decay photons propagate without scattering, while the dashed line indicates the bound for particles of mass $> 10^5(\tau_x/t_0)^{\frac{2}{3}}$ GeV whose decay photons trigger radiation cascades on the 2.7 ^{0}K radiation.

Figure 6. Upper bounds on the decaying particle abundance as a function of its lifetime from limits on upward-going muons (full lines) and contained events (dashed lines) in the *IMB* detector, and from the limit on high energy air showers obtained by *Fly's Eye* (dot-dashed line). The lines are labelled by the mass of the particle being considered. The right-hand scale, which is applicable only for lifetimes $\tau_x > t_0$, shows the present energy density of the particle; the horizontal line indicates the observational bound $\Omega_x h^2 < 1$. The bounds shown in figs. 3, 4 and 5 are also displayed (dotted lines) for comparison. The hatching delimits the region allowed for particles with mass ~ 1 TeV: the region allowed for particles weighing $\sim 10^{10}$ GeV is slightly larger for $\tau_x \gtrsim t_0$.

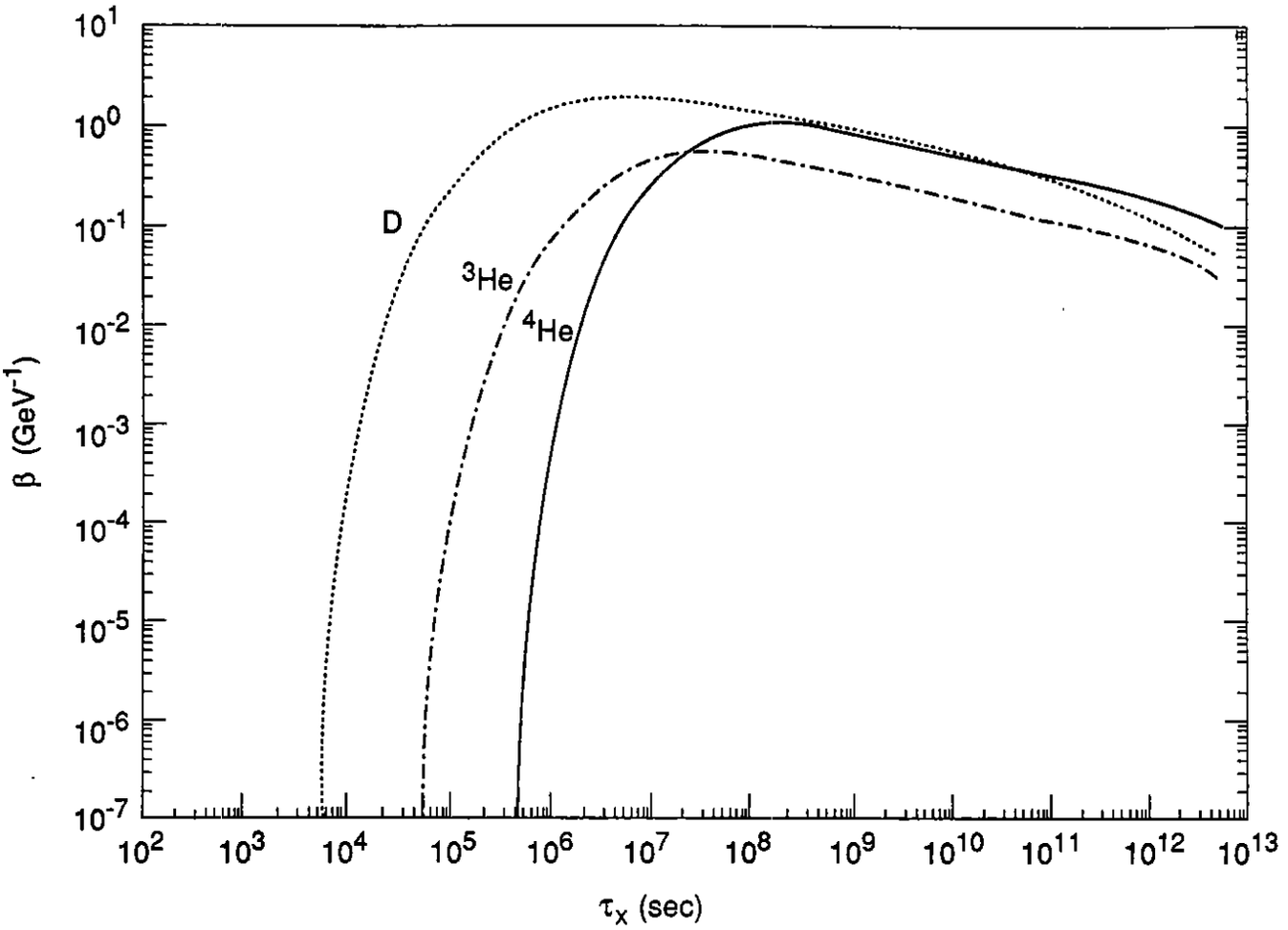

- Figure 2 -

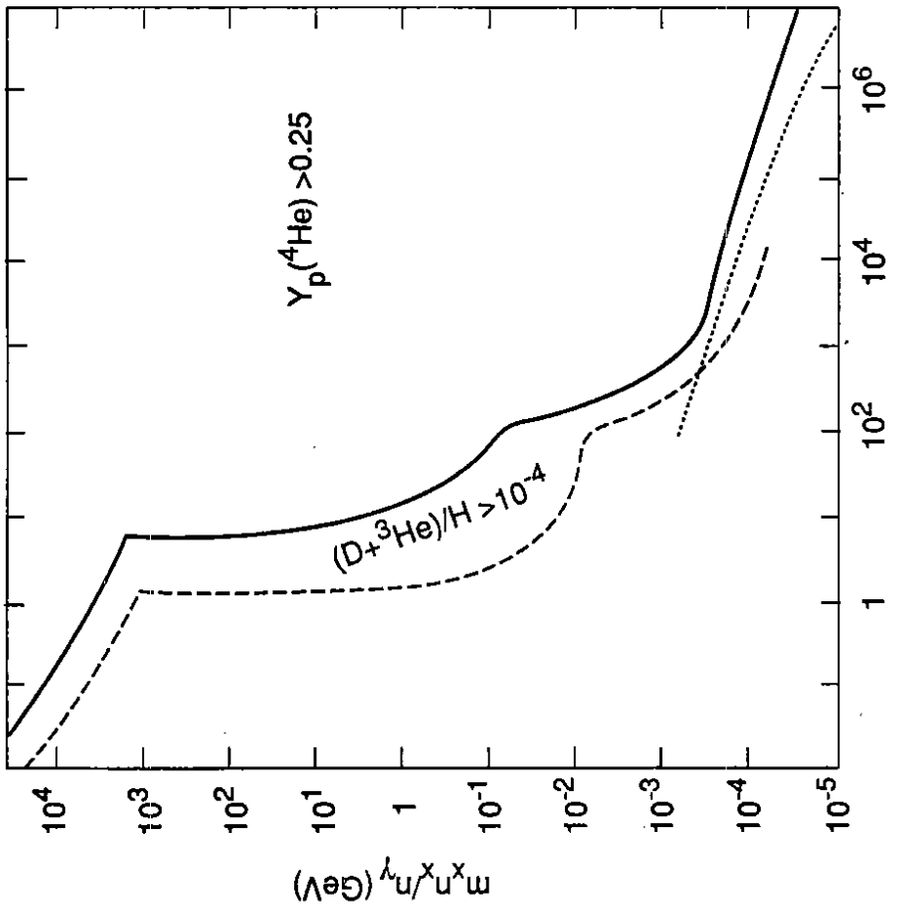

- Figure 1 -

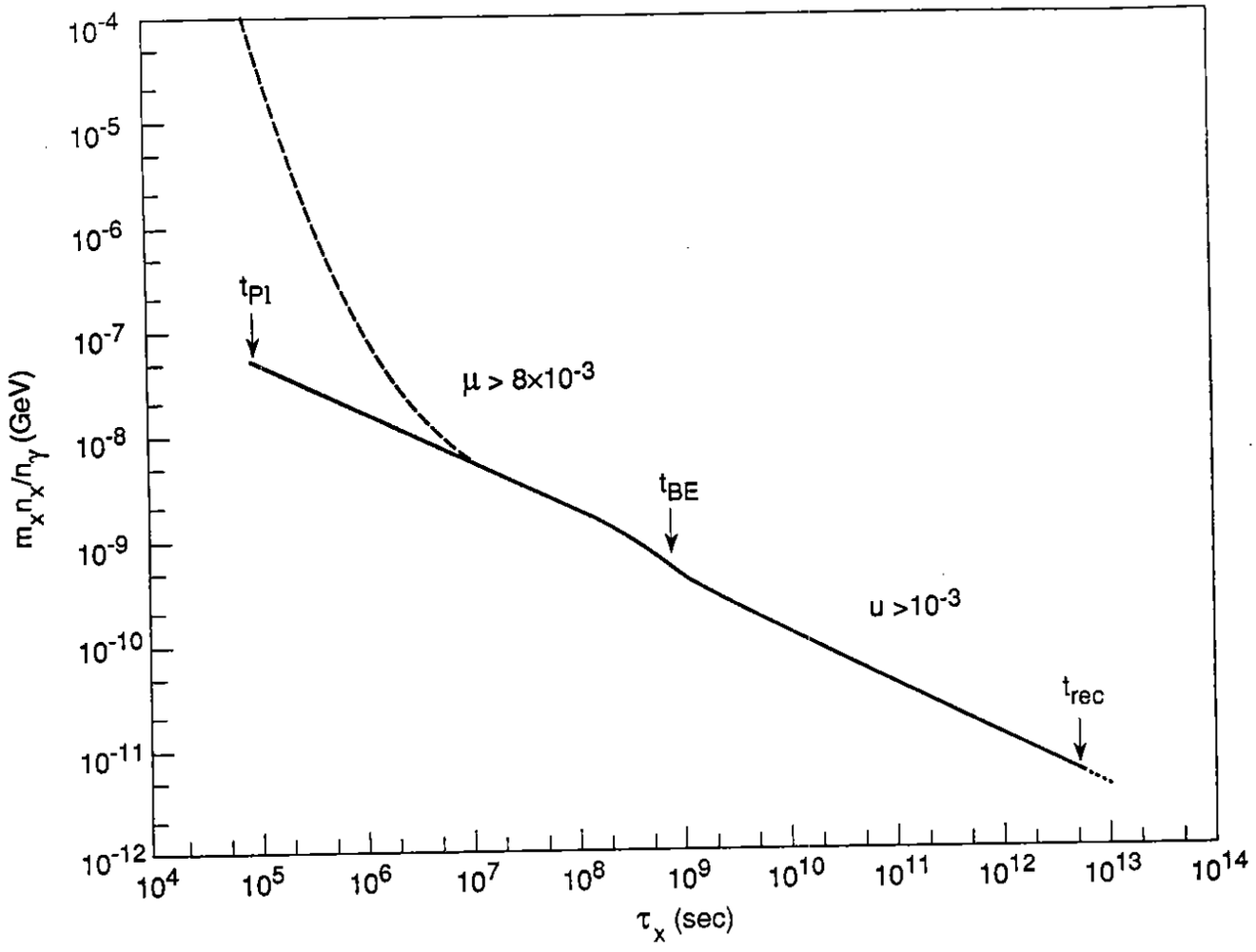

- Figure 4 -

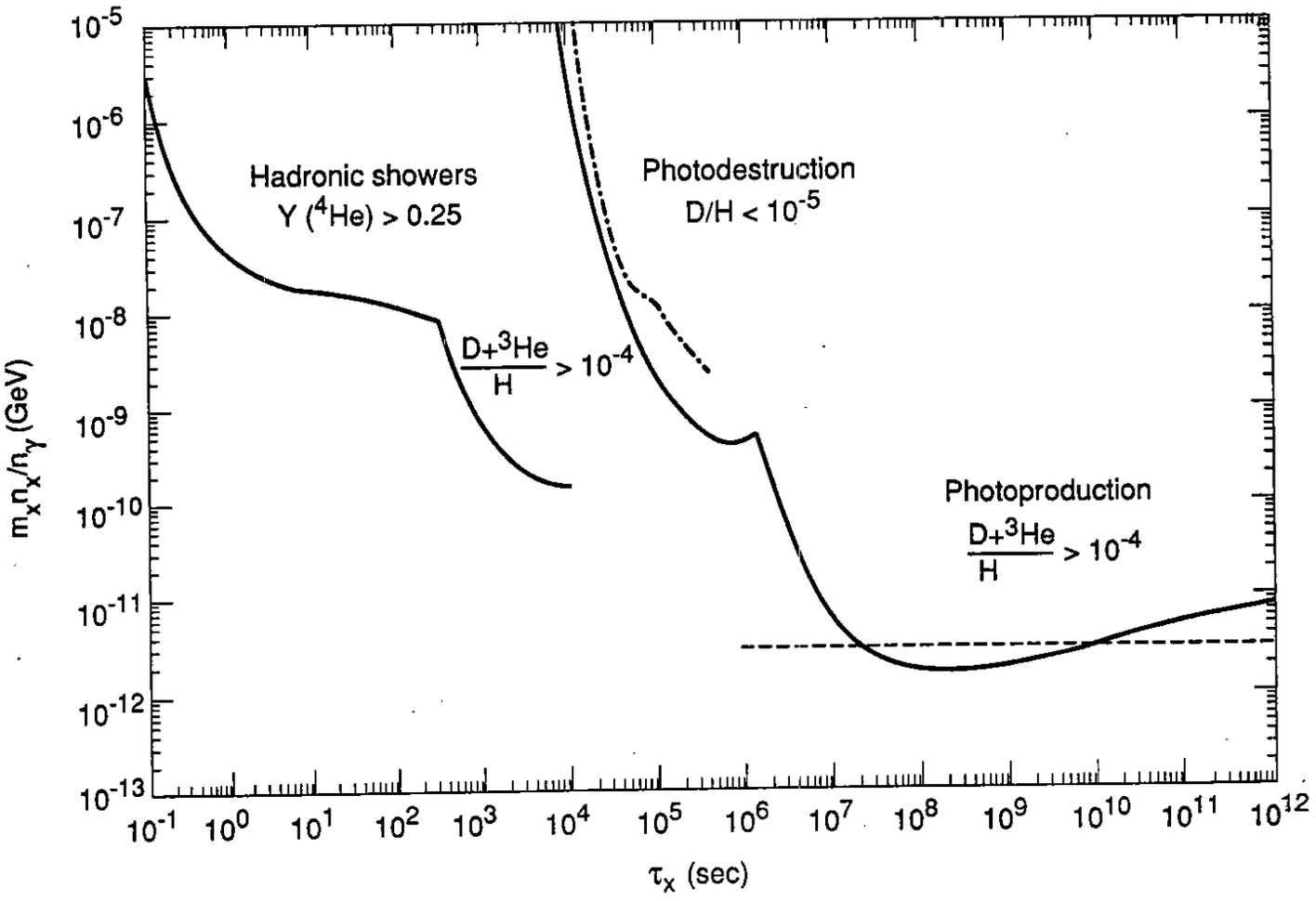

- Figure 3 -

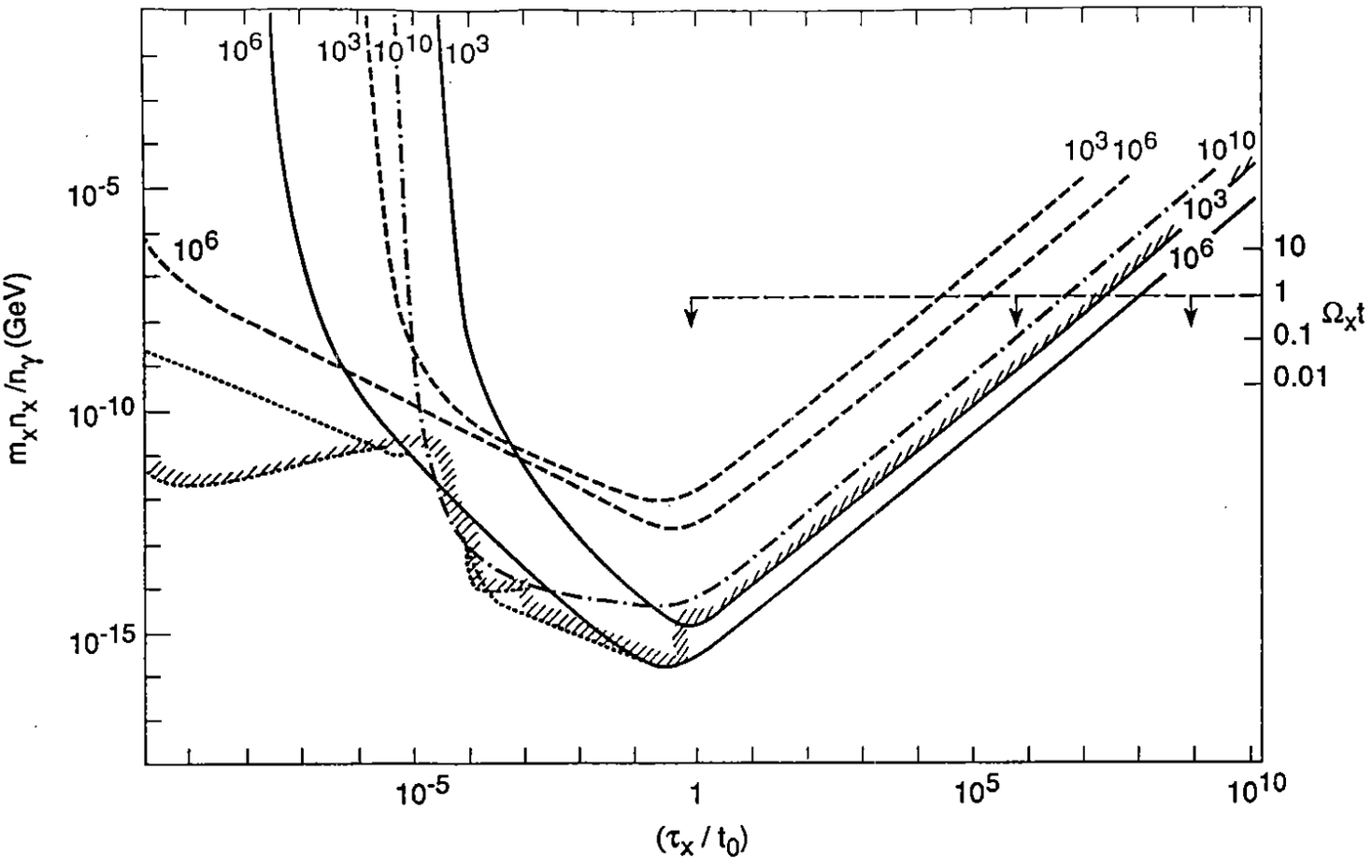

- Figure 6 -

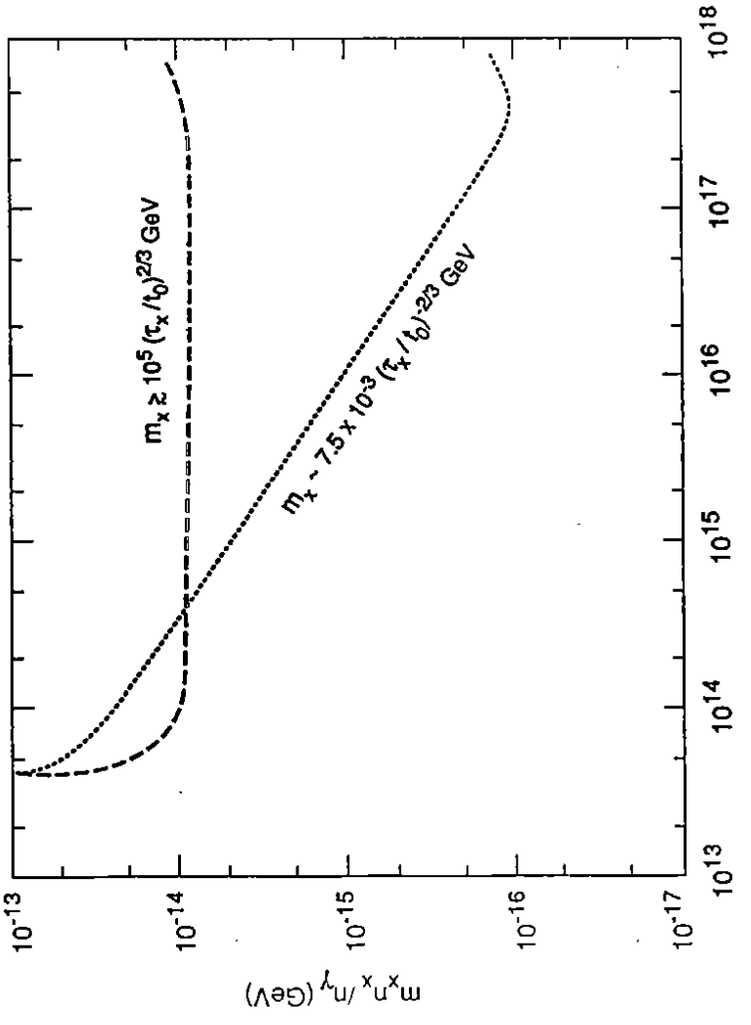

- Figure 5 -

Imprimé au CERN. Prix: 0.65 Fr.